Trends in Flooding in Europe and North America - an Extreme Value Approach

Axel Ström

September 18, 2018

Abstract

This study examines minimally altered catchments in Europe and North America in order to determine whether any changes to the dynamics of flooding have occurred due to changes in the climate. By examining the parameters of the Generalized Extreme Value (GEV) distributions of individual catchments it is possible to determine not just if changes in flood patterns have occurred, but also the nature of these changes. The main conclusion of the study was that the scale parameters of catchments in North America have increased over time. The effects on return levels, however, were inconclusive, where despite significant individual trends, no global or regional patterns were found.

Acknowledgement

This thesis would not be what it is today without the help from several people. First of all I want to extend my thanks and gratitude to my supervisor Nader Tajvidi for all his help with the project. I also want to thank James Hakim for his help with making the interactive maps accessible.

I also want to thank my friends for their support, and the Department of Statistics for giving me a place to work.

Contents

1 Introduction **4**

2 Theory **4**

3 Data and Methods **7**
3.1 Data 7
3.2 Method 12
3.2.1 Overview of method 12
3.2.2 Detailed method 12
3.2.3 Motivation of Method 13
3.3 Inference 15

4 Results **16**
4.1 Analysis of data from 1961-2010 16
4.1.1 Simple model 16
4.1.2 Full model 19
4.2 Analysis of data from 1931-2010 22
4.2.1 Simple model 22
4.2.2 Full model 25
4.3 Conclusions 29

5 Summary and Concluding Remarks **31**

A Distributions and tests **I**

B Box plots of the estimated median **II**
B.1 1961 data, simple model II
B.2 1961 data, full model III
B.3 1931 data, simple model VI
B.4 1931 data, full model VII

1 Introduction

Large floods cause enormous damages each year. Gaining a better understanding of how the patterns of flooding change over time is important in order to better plan and mitigate these risks. Of particular interest is the effects on flooding stemming from the increasing air temperatures caused by climate change. Based on several regional studies, the Intergovernmental Panel on Climate Change (IPCC) found no evidence of a global trend in either frequency and magnitude of flooding [8][p. 214].

In a study by Hodgkins et al. [9] a larger number of minimally altered catchments across Europe and North America were investigated. Their study focused on major floods, modeling exceedances over the 25, 50, and 100-year return levels, finding no evidence of regional or global trends in major flood occurrence. This study aims to expand on their study by modeling the same data, but instead focus on whether the parameters of the Generalized Extreme Value (GEV) distribution for each catchment exhibit any trends.

The results from this study were that there is a significant change in the GEV parameters over time. Most prominently, this included an increased scale parameter over time in North America, as well as some indications of a decreasing scale parameter in Europe. The resulting estimated median return levels however, were inconclusive, with no regional or global patterns found. This suggest that for return levels, a local or individual approach may be better than a regional or global approach.

The structure of this study is as follows. In Section 2 an overview of the relevant theory is given, defining the distributions and tests, as well as giving an introduction to extreme value theory. In Section 3 an overview of the data as well as the method is presented. In Section 4 the results of the analysis are presented. Finally, in Section 5 a quick summary of the study is given as well as suggestions for further research.

2 Theory

The main focus of this study is to use extreme value theory to model flood occurrence. A brief introduction to the field of extreme value theory is therefore in order. In addition, some useful tests and distributions are defined in Appendix A.

The primary interest of extreme value theory is to model the most extreme values of a sequence of random variables. The most natural approach is to examine the maximum of the sequence. Let $X_1, \ldots, X_n$ be a sequence of independent and identically distributed random variables, with some distribution function F. The maximum of this sequence is defined as $M_n = \max(X_1, \ldots X_n)$. From this, the distribution function of M_n can be

formed:

$$\begin{aligned} P(M_n \leq z) &= P(X_1 \leq z, X_2 \leq z, \dots X_n \leq z) \\ &= \prod_{i=1}^{n} P(X_i \leq z) \\ &= F^n(z) \end{aligned}$$

From this, it would be possible to estimate the distribution function of M_n by estimating F from the data. However, small errors in the estimate of F lead to much larger errors in the estimate of F^n. Instead, we can further examine the behavior of F^n when n becomes very large.

$$\lim_{n\to\infty} F^n(z) = \begin{cases} 0, & z < z_+ \\ 1, & z \geq z_+ \end{cases}$$

where z_+ is the upper end-point of F. In other words, the distribution function is degenerate. In order to avoid this, M_n can be normalized as:

$$M_n^* = \frac{M_n - b_n}{a_n}$$

For sequences of constants, $a_n > 0, b_n \in \mathbb{R}$. If chosen appropriately, the distribution of M_n^* will be max-stable, see Definition 2.1.

Definition 2.1 (Max-stable) *Let $X_1, X_2, \dots, X_n$ be independent and identically distributed random variables with some distribution function F.*

If there exist sequences $a_n > 0, b_n \in \mathbb{R}, \forall n \in \mathbb{N}$:

$$F^n(a_n z + b_n) = F(z) \qquad \forall z \in \mathbb{R}$$

then the distribution of X is max-stable [10]

The following theorem (Theorem 2.1) is perhaps the most important theorem in all extreme value theory, as it provides limiting distributions for max-stable distributions.

Theorem 2.1 (Fisher-Tippett-Gnedenko) *Let $X_1, X_2, \dots, X_n$ be independent and identically distributed random variables and define $M_n = \max(X_1, \dots, X_n)$. If there exist sequences $a_n > 0, b_n \in \mathbb{R}, \forall n \in \mathbb{N}$:*

$$P\left(\frac{M_n - b_n}{a_n} \leq z\right) \to G(z) \qquad as \;\; n \to \infty$$

for a non-degenerate distribution function G,
then G belongs to one of the following families of distributions:

I The Gumbel family:

$$G(z) = \exp\left[-\exp\left(-\frac{z-b}{a}\right)\right]$$

II The Fréchet family:

$$G(z) = \begin{cases} 0, & x \leq b \\ \exp\left[-\left(\frac{z-b}{a}\right)^{-a}\right], & z > b \end{cases}$$

III The Reversed Weibull family

$$G(z) = \begin{cases} \exp\left\{-\left[-\left(\frac{z-b}{a}\right)^{a}\right]\right\}, & x < b \\ 1, & z \geq b \end{cases}$$

The three families of distributions in Theorem 2.1 can be reformulated to the generalized extreme value distribution using Theorem 2.2.

Theorem 2.2 (Extreme Value Theorem) *Let $X_1, X_2, \ldots, X_n$ be independent and identically distributed random variables and define $M_n = \max(X_1, \ldots, X_n)$. If there exist sequences $a_n > 0, b_n \in \mathbb{R}, \forall n \in \mathbb{N}$:*

$$P\left(\frac{M_n - b_n}{a_n} \leq z\right) \to G(z) \qquad as \;\; n \to \infty$$

for a non-degenerate distribution function G,
then G belongs to the GEV family:

$$G(z) = \exp\left[-\left(1 + \gamma\frac{z-\mu}{\sigma}\right)^{-1/\gamma}\right]$$

defined on $z : 1 + \gamma\frac{z-\mu}{\sigma} > 0$, where $\mu \in \mathbb{R}$, $\sigma > 0$, $\gamma \in \mathbb{R}$ [5]

In the representation in Theorem 2.2, the Gumbel family correspond to $\gamma = 0$, the Fréchet family to $\gamma > 0$, and the Weibull family to $\gamma < 0$. In the above representation, μ is called the location parameter, σ is called the scale parameter, and γ is called the shape parameter.

Even though the normalizing constants are unknown in practice, this presents no problem. If, for some sufficiently large n,

$$P\left(\frac{M_n - b_n}{a_n} \leq z\right) \approx G(z)$$

Then this can easily be rewritten as:

$$\begin{aligned} P(M_n \leq z) &\approx G\left(\frac{z - b_n}{a_n}\right) \\ &= G^*(z) \end{aligned}$$

where G^* is a member of the GEV family. Thus there is no need to estimate the normalized maxima. [5]

Based on the GEV distribution, return levels can be calculated as follows.

Theorem 2.3 (Return levels) *If X is a GEV-distributed random variable with ML estimated parameters $\hat{\mu}, \hat{\sigma}$, and $\hat{\gamma}$. Then, the ML estimate of the m-year return level, $\hat{x}_m$ can be found as:*

$$\hat{x}_m = \hat{\mu} - \frac{\hat{\sigma}}{\hat{\gamma}}\left\{1 - [-\log(1 - 1/m)]^{-\hat{\gamma}}\right\} \qquad \text{for } \gamma \neq 0.$$

The GEV distribution can also be extended to allow its parameters to change over time. This is especially useful when modeling non-stationary series, and will be used extensively in this study. For details on how this extension is made, see Coles [5, p.106-107].

3 Data and Methods

This section is divided into three parts. In the first part, the data, as well as the analytical tools used, is discussed. In the second part, a detailed overview of the method employed will be presented. Finally, the inference methods are explained.

3.1 Data

The data used for this study is the data provided by Hodgkins et al. [9], which should ensure a good comparability between the studies. The data consists of the yearly maximum waterflow of each of the catchments, as well as the coordinates of each catchment. To illustrate the nature of this data, a scatter plot showing the annual maximum waterflow at Saint John River in Canada is shown below in Figure 1.

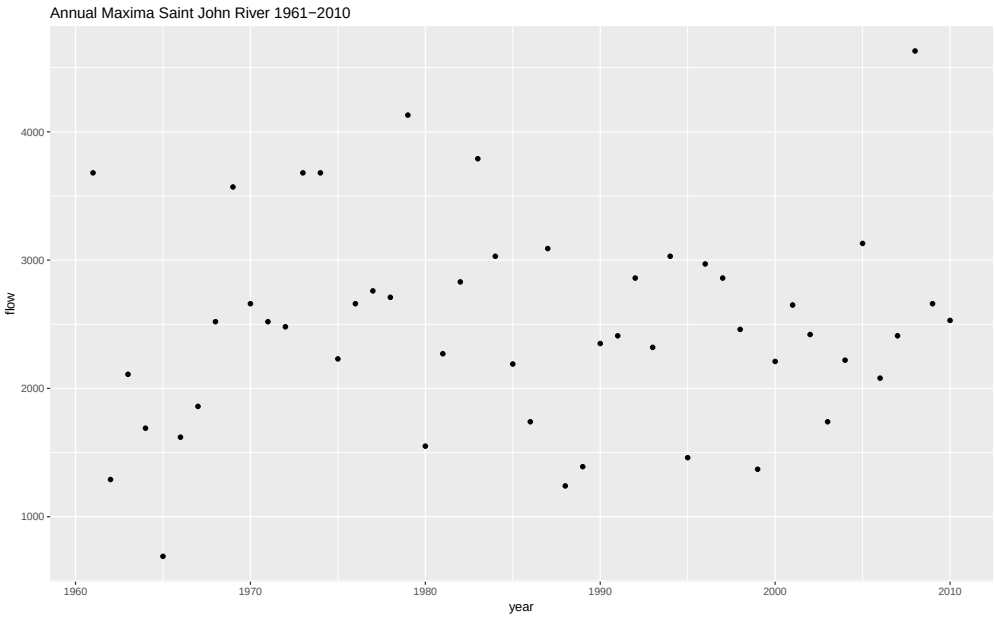

Figure 1: Annual maxima at Saint John River, Canada.

The data set consists of two parts, the first containing observations from 1204 catchments from 1961-2010. The second part includes observations of 322 catchments from 1931-2010. A map showing the location of the catchments with data available from 1961 is found in Figure 2. The corresponding map for the catchments with data available from 1931 is found in Figure 3

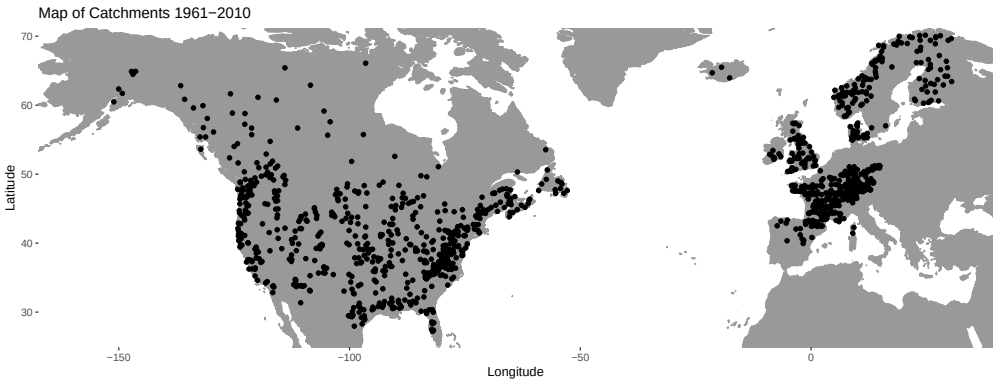

Figure 2: Catchments 1961-2010.

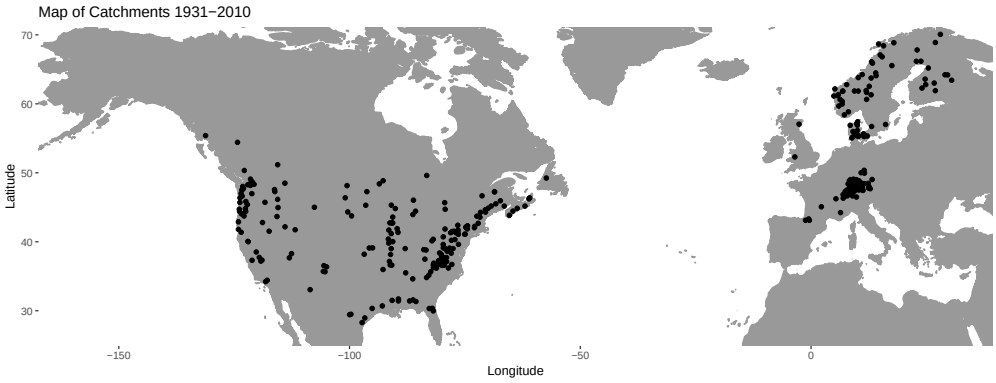

Figure 3: Catchments 1931-2010.

In addition to time, ocean-atmosphere indices have been suggested to influence flooding. In particular the Atlantic multidecadal oscillation (AMO)

index [6] and the Pacific decadal oscillation index (PDO) [9]. Monthly unsmoothed values have been obtained from `https://www.esrl.noaa.gov/psd/data/climateindices/list/`. The monthly values were converted to yearly values by averaging the values from October to the following September. This corresponds to the method used by Hodgkins et al.[9]. The resulting time series for the AMO is found in Figure 4, and the series for the PDO is found in Figure 5.

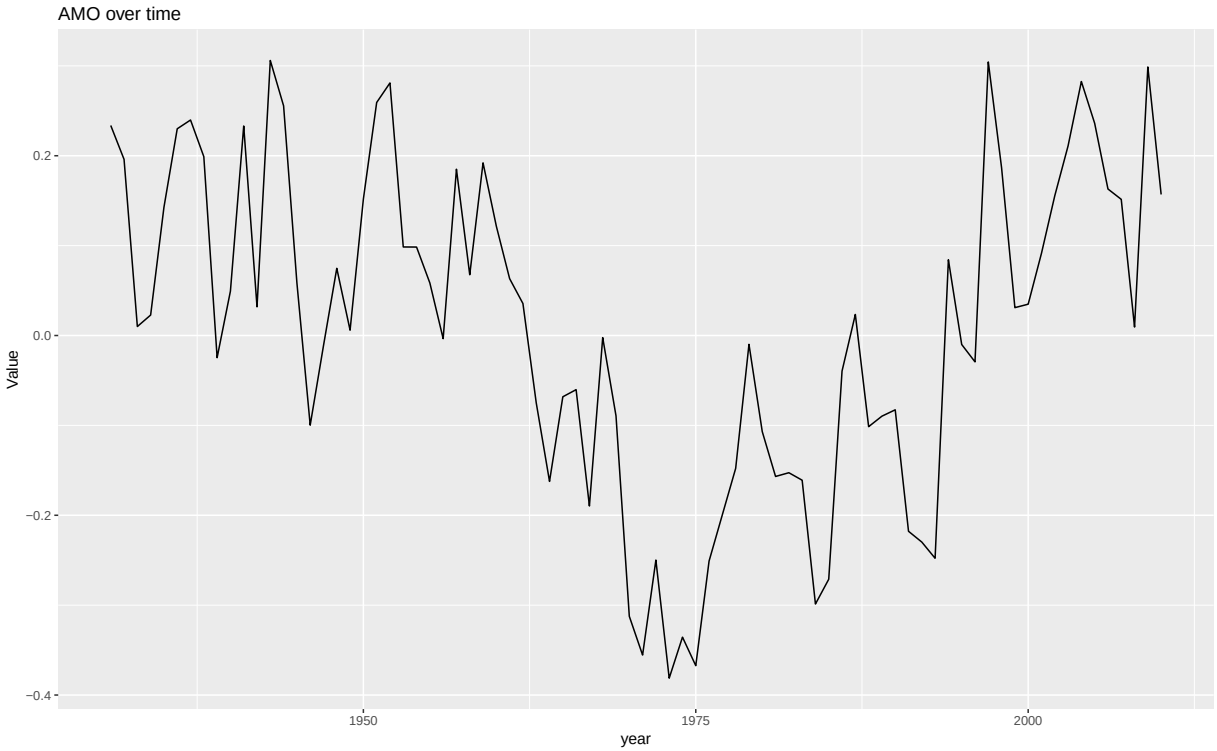

Figure 4: AMO 1931-2010

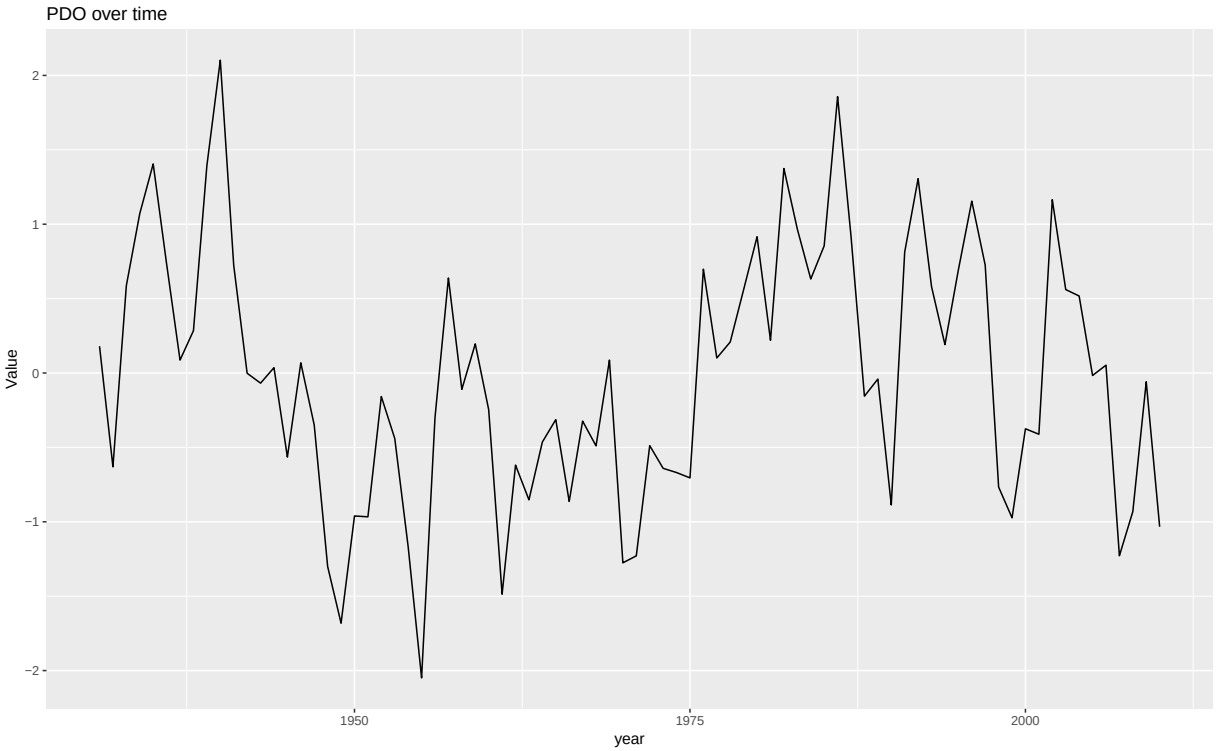

Figure 5: PDO 1931-2010

In order to ensure numerical stability when fitting GEV distributions, the year, AMO, and PDO have been linearly rescaled so that the minimum value corresponds to 0 in the new series, and the maximum corresponds to 1. The data set has also been divided into two parts, one part where AMO was deemed more likely to influence the occurrence of floods, and one part where PDO was deemed more likely. For simplicity's sake, this split was chosen to be a vertical line at 108° west. The catchments west of this split use PDO as a covariate, while the catchments east use AMO as a covariate.

Since Hodgkins et al. [9] only found a relationship between flooding and AMO, AMO was also used as a covariate for all catchments in a separate study. The results of that study are not shown here, but agree with the results presented here with only very minor differences.

The statistical analysis was done using R [12]. A number of R packages have been used. For the maps used to generate the plots in this paper `mapdata` [4] was used. For all graphical plots `ggplot2` [13] was used. For the interactive maps accompanying this paper, `mapview` [1] and `webshot` [2] was used.

For all fitting of GEV functions, the maximum likelihood method of the R package `extRemes` [7] was used. When fitting distributions for a catchment, years with missing values were ignored.

3.2 Method

3.2.1 Overview of method

The method used in this study has been developed with three goals in mind. The first goal is that the results shall be comparable to the results obtained by Hodgkins [9]. Therefore the same data set is used, and the Atlantic Multidecadal Oscillation (AMO) and Pacific Decadal Oscillation (PDO) indices are chosen as covariates. The second goal is to allow for several different post hoc groupings of the catchments. This is achieved by treating the catchments individually, rather than grouping them. The third goal is to determine if the addition of a trend is a significant contribution to the overall performance of the model.

The method consists of five main steps. First, as previously mentioned, the data was split into two sets. Then, for each set, the optimal GEV distribution without any trends is fitted to each catchment. Thirdly, this model is extended by adding a trend component. Thereafter, these models are compared, and a Likelihood Ratio test is performed to see if the model is significantly improved by adding the trend. Finally, the calculated number of significant trends is compared to the theoretical number according to the null hypothesis.

3.2.2 Detailed method

When fitting the optimal GEV distribution without trends, three GEV distributions are fitted, one base fit without any covariates, one where the location parameter is dependent on the covariate (AMO or PDO depending on the data set), and one where the natural logarithm of the scale parameter is dependent on the covariate. Then Likelihood Ratio tests are used to determine if either extended model is better than the base fit.

If neither extended model is significantly better than the base fit, the base fit is chosen as the best model without trends. If only one extended model is significantly better, then that model is chosen. If both extended models are better than the base fit a fourth fit is computed, where both the location and the logarithm of the scale parameters are dependent on the covariate. Then this model is tested against both of the extended models using Likelihood Ratio tests. If it is significantly better than both extended models, it is chosen. Otherwise it is rejected and the extended model with the lowest AIC is chosen.

When adding the trend component, the approach is very similar to the above method. However, instead of using a base model with no covariates, the previously selected model is used. Then it is extended by adding time as a covariate for either the location or the scale parameter. Then, using the same logic as before, Likelihood Ratio tests are used to determine if this has

improved upon the base model. If neither extended model is significantly better, the base model is selected, and there is no evidence that there is a trend for this particular catchment. If only one extended model is significantly better, that model is chosen as the final model. If both extended models provide a significant improvement, a new model is fitted, where time is treated as a covariate for both the location parameter and the scale parameter. Then, once again using Likelihood Ratio tests, if this is better than both extended models, it is selected as the final model. Otherwise, the extended model with the lowest AIC is selected. Note that any model other than the base model is dependent on time, and therefore evidence for a significant trend for that particular catchment.

A separate analysis was also conducted, henceforth called the simple model, where only time is considered a covariate. This model follows the same method as before, using a base fit without any covariates when fitting the best model with a trend.

To illustrate the effects on changes in the parameters of the GEV distribution, the estimated median (i.e. the 2-year return level) water flow has been calculated for each catchment and year, as well as a predictions for the median from 2010 to 2045. For those catchments which exhibit no trend in either AMO/PDO or time, this will be stationary and unaffected by time. For the other catchments, however, this will vary over time. The median is chosen since the sign of γ varies between the catchments, and choosing the median rather than the left/right end-point allows for a comparison of all catchments, since the mean is not always exist for fitted GEV distributions.

For future values of the AMO/PDO, previous values with a delay of 70 years were used, in accordance to their long term periodicity [3], [11]. This is a very crude method, but it serves well for the purpose of illustrating the effects of changing time. The results will be presented as box plots for the estimated median each year for each of the catchments with significant trends, either in AMO/PDO or time (or both). There are separate plots for each combination of model, continent, and type of interaction. In general, for each model, only one plot is shown if the results are similar across both Europe and North America, as well as across type of interaction. All box plots are found in Appendix B.

3.2.3 Motivation of Method

With regards to choosing a method, several important considerations were made. By modeling the parameters of the GEV distribution itself as compared to conducting inference on return levels, we lose no information. It is possible that two completely different GEV distributions have the same return level. To illustrate this, two different GEV distributions are shown in Figure 6. It is obvious that despite the same 25-year return level, marked

by the vertical dotted line, the distributions exhibit totally different characteristics, especially in the tail of the distributions. Despite having the same 25-year return level, the dashed line distribution has a larger 100 -year return level.

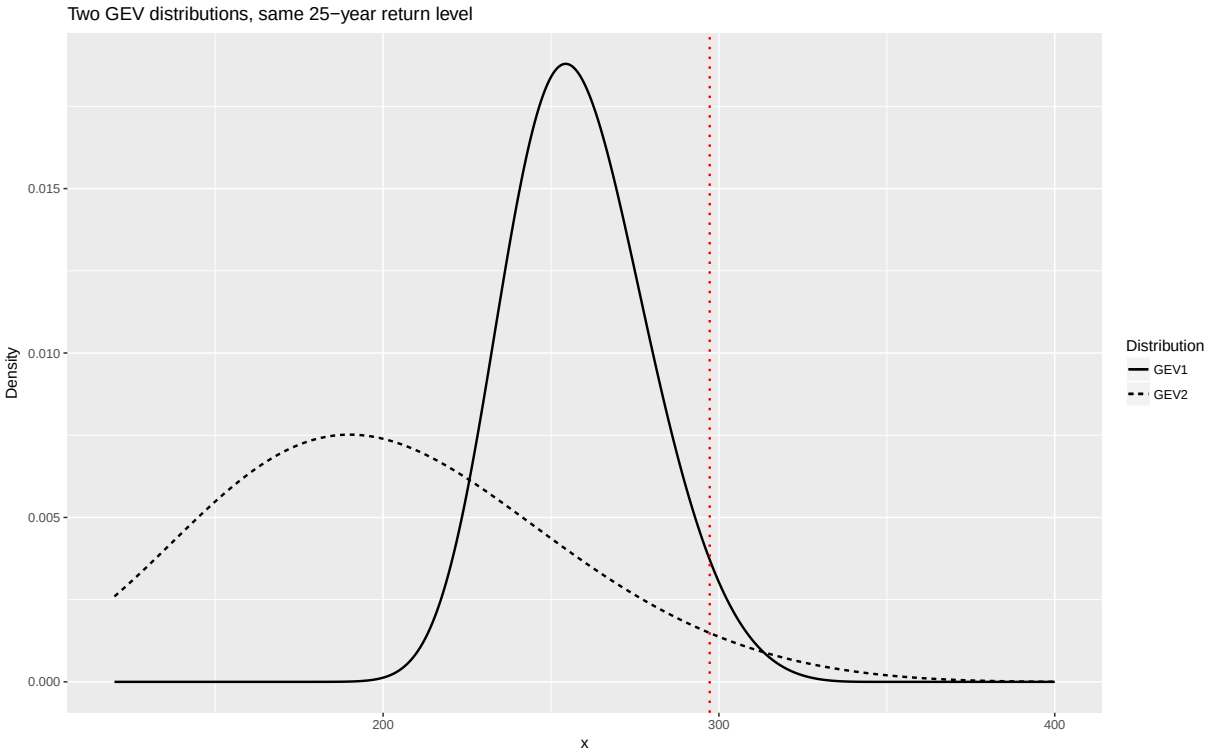

Figure 6: Illustrative example
Two GEV distributions with different parameters, but same 25-year return level. The parameters of GEV1 are $\mu = 250, \sigma = 20, \gamma = -0.2$. The parameters for GEV2 are $\mu = 179.1171, \sigma = 50, \gamma = -0.2$. The dotted line represents the 25-year return level

Another advantage of examining the parameters of the GEV distribution is that it allows us to treat each catchment separately, thus eliminating the problem with flood dependence in time and space encountered by Hodgkins et al. [9]. By treating the catchments separately, there is no risk of incorrectly grouped catchments affecting the analysis; all grouping of catchments can be done post hoc. In this study, the only grouping has been based on continent, but it is possible to break down the results further into groups similar to the groups used by Hodgkins [9] to achieve a direct comparison with their results.

Another important consideration is adding the trend at the last possible moment. By doing so, one can see if it contributes something that cannot be explained by the ocean-atmosphere indices. If the trend contributes

something even after all other explanatory factors are considered, it strongly indicates that the trend is an essential part of understanding major flood occurrence.

3.3 Inference

The main goal of this study is to answer the question of whether or not time makes a meaningful contribution to the understanding of the occurrence of major floods. Therefore the following hypotheses have been proposed.

$$H_0 : \text{No catchments are affected by trends}$$
$$H_1 : \text{At least one catchment is affected by trends}$$

To investigate this, a test function must be created. By selecting a suitable confidence level when fitting the models containing trends, one can achieve such a function. Since there are multiple models tested, one must first select the total significance level desired, and from there work out the individual significance levels needed to achieve this level. In this case, there are two models we are testing, which when all significance levels are chosen to be equal, gives:

$$\begin{aligned} \alpha_{total} &= \alpha_1 * \alpha_2 \\ \alpha_{total} &= \alpha^2 \\ \alpha &= \sqrt{\alpha_{total}} \end{aligned}$$

So, if a final significance level of 0.95 is desired, the significance level applied to the LR tests is $\sqrt{0.95}$. Then, under the null hypothesis, the number of catchments, x, where the trend is significant will be binomially distributed as:

$$x \sim Bin\,(n, 0.05)$$

where n is the number of catchments examined. Based on this, p-values can be obtained by comparing the calculated number of significant trends to the theoretically expected value. Using a normal approximation, confidence intervals can also be constructed.

Finally, for all significant trends, it is also of interest to examine the effect of the trend. To do so, the following hypotheses are formulated:

$$H_0 : \text{Time affects the parameter equally in both directions}$$
$$H_1 : \text{Time affects the parameter more in one direction}$$

Thus, under the null hypothesis, the probability that time would have a negative effect on the given parameter, provided that the trend is significant, would be 0.5. The total number of times, y, where time has a negative effect on the parameter is then binomially distributed as:

$$y \sim Bin\,(k, 0.5)$$

where k is the number of significant trends for the given parameter. Since the distribution under the null hypothesis is known, p-values can be calculated.

4 Results

In addition the the results presented in this section, four interactive maps have been generated, showing all estimated parameters for each catchment, data set, and model. These maps are available to download at `http://ctr.maths.lu.se/matstat/exjobb/maps`.

4.1 Analysis of data from 1961-2010

4.1.1 Simple model

The results from the simple model for the short time series is presented in Table 1. The simple model indicates clearly that the trend cannot be ignored when modeling flood occurrences. One must be wary when interpreting these results however, since the simple model does not take the AMO and PDO into account. This could result in mistakenly identifying a trend, rather than the effect of the AMO or PDO. This risk is further increased for the short time series, since it is shorter than the periodicity of the AMO, which is around 70 years [3]. The same holds true for the PDO, which has a periodicity of between 50 and 70 years [11]

Table 1: Results from the Simple Model 1961-2010

	# of catchments	# of significant trends	p-value	95% CI LB	95% CI UB
Europe	559	91	<2.2e-16	0.1322	0.1932
North America	645	64	2.3247e-7	0.0762	0.1223
Total	1204	155	<2.2e-16	0.1098	0.1477

A map with the catchments with significant trends can be found in Figure 7 with the dark dots representing catchments where significant trends were

found, and the light dots represents catchments where no such trend was found.

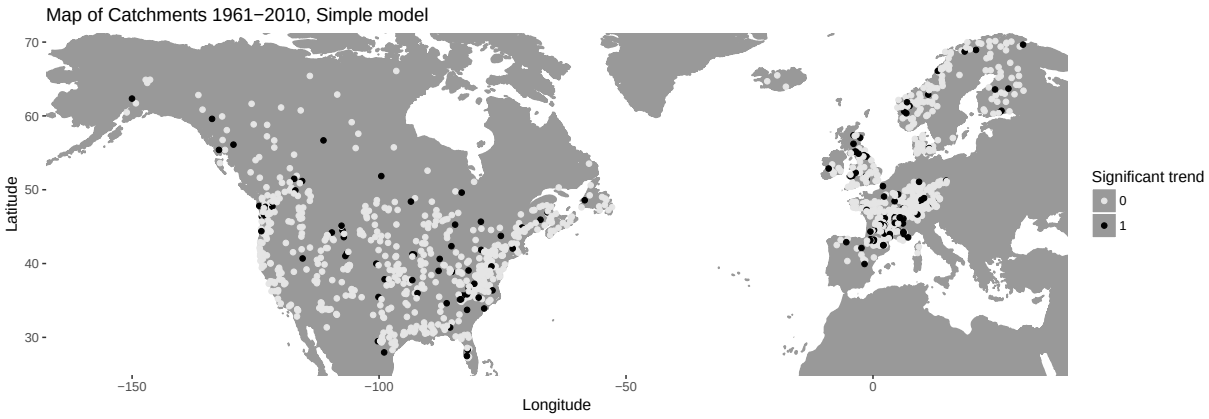

Figure 7: Significant catchments 1961-2010, simple model

A summary of the effects of the trends is found in Table 2. As before, when interpreting this table, caution is needed. Based on this table, it is hard to say whether there are any clear conclusions regarding the direction of the trend in location. Regarding the trend in scale however, it appears that over time, the scale parameter increases, particularly in North America. In fact, the probability of achieving such a result if the trend affected the scale parameter equally in both directions is 0.0005.

Table 2: Simple model 1961-2010, direction of trends

	Increasing μ	Decreasing μ	Increasing σ	Decreasing σ
Europe	25	35	21	12
North America	14	25	21	4
Total	39	60	42	16

The effect of the significant trends on the parameters of the GEV. Note that the number of effects are greater than the number of significant trends, since for some catchments the trend affected both the location and scale parameters

The estimated median for the catchments in North America that had a significant relationship with time in their parameters are shown in Figure 8. For the individual catchments, such as the outliers, the effects are clear and easy to interpret. When looking at all catchments together, however, there are no apparent conclusions. It appears that each catchment's median return level is affected differently. Thus, there are no clear trends for all catchments. The same holds true for the European catchments. All box plots for the simple model using the 1961-2010 data set can be found in Appendix B.1.

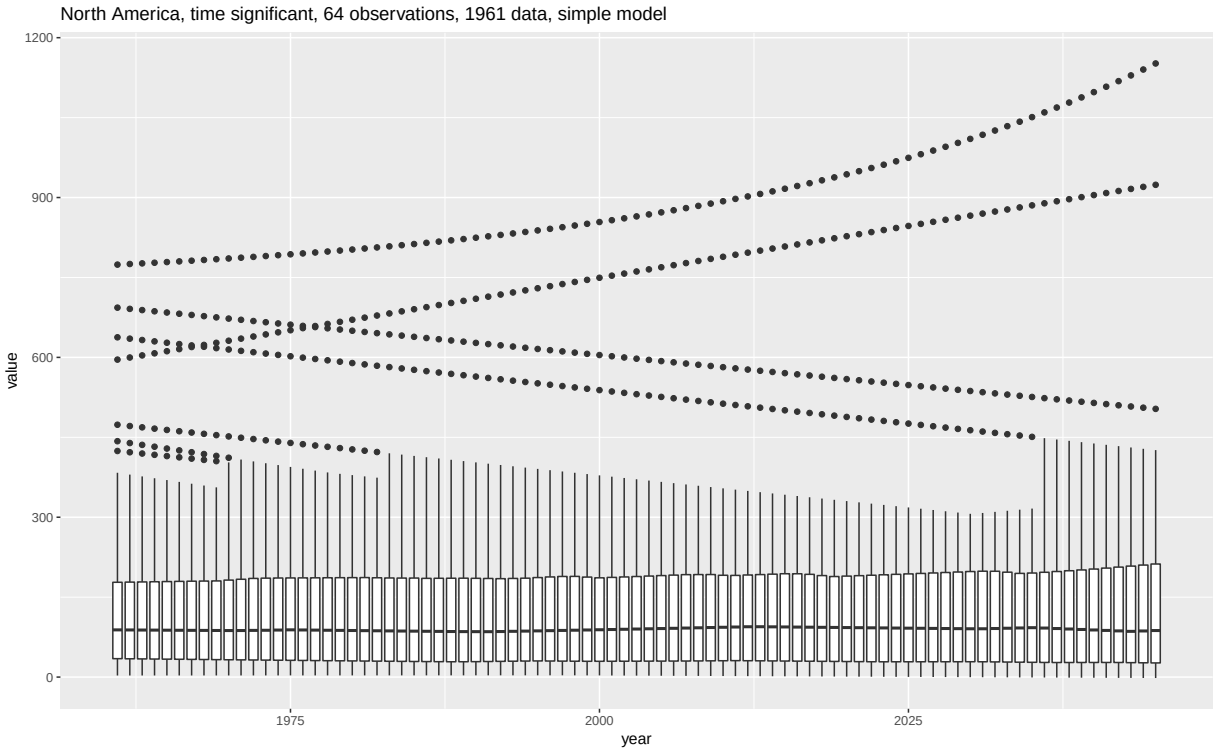

Figure 8: Box plot of the median, simple model

The estimated median by year for the catchments in North America with a significant trend in time, using the simple model for the 1961-2010. This corresponds to 64 catchments in total.

4.1.2 Full model

The results for the full model are shown below, in Table 3. As expected, when AMO and PDO are introduced, there are fewer catchments with significant trends. Despite this, the number of significant catchments is significantly higher than what would be expected under the null hypothesis. This means that there is significant evidence that there is a trend influencing the dynamics of flood occurrence.

Table 3: Results from the Full Model 1961-2010

	# of catchments	# of significant trends	p-value	95% CI LB	95% CI UB
Europe	559	54	4.1937e-6	0.0721	0.1211
North America	645	47	0.0072	0.0526	0.0929
Total	1204	101	4.7629e-7	0.0682	0.0995

A map with the catchments with significant trends can be found in Figure 9. There are no major differences compared to Figure 7. There are no obvious geographical patterns in how the significant catchments are distributed.

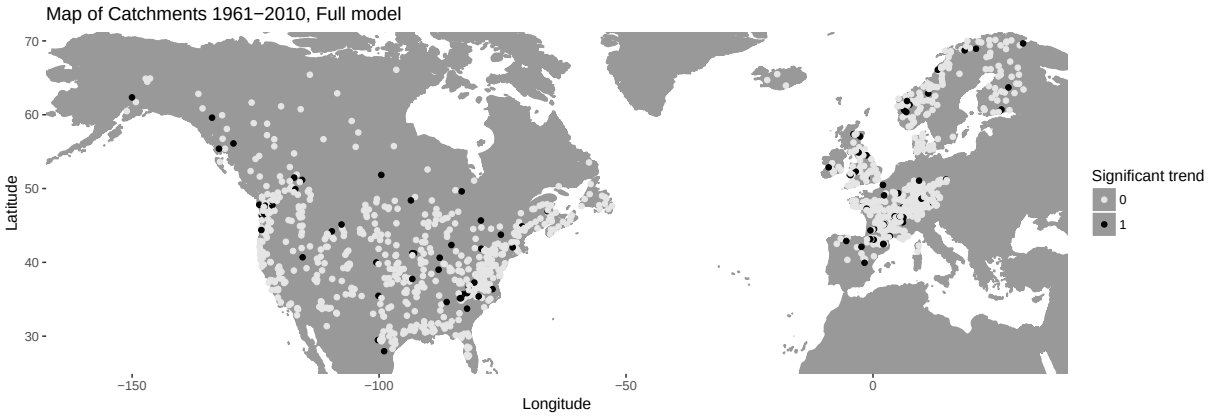

Figure 9: Significant catchments 1961-2010, full model

The effects of the trend on the parameters of the GEV distributions for the full model can be found in Table 4. Once again, there are no clear effects on the location parameter. There no longer appears to be an effect on the scale parameter in Europe, however the scale parameter for North America is still significantly positively affected by the trend (p-value 0.0021).

Table 4: Full model 1961-2010, direction of trends

	Increasing μ	Decreasing μ	Increasing σ	Decreasing σ
Europe	17	18	13	10
North America	13	18	14	2
Total	30	36	27	12

The effect of the significant trends on the parameters of the GEV. Note that the number of effects are greater than the number of significant trends, since for some catchments the trend affected both the location and scale parameters

The estimated median for the catchments in North America that had a significant relationship with time in their parameters are shown in Figure 10. The results are very similar to the results of the simple model, namely that for individual catchments, the trend can be observed, but there doesn't appear to be any trends for all the catchments. The results are similar when looking at those catchments which had a relationship with both AMO/PDO and time, and those that only had a relationship with AMO/PDO. The European catchments exhibit the same pattern. All box plots for the full model using the 1961 data set can be found in Appendix B.2.

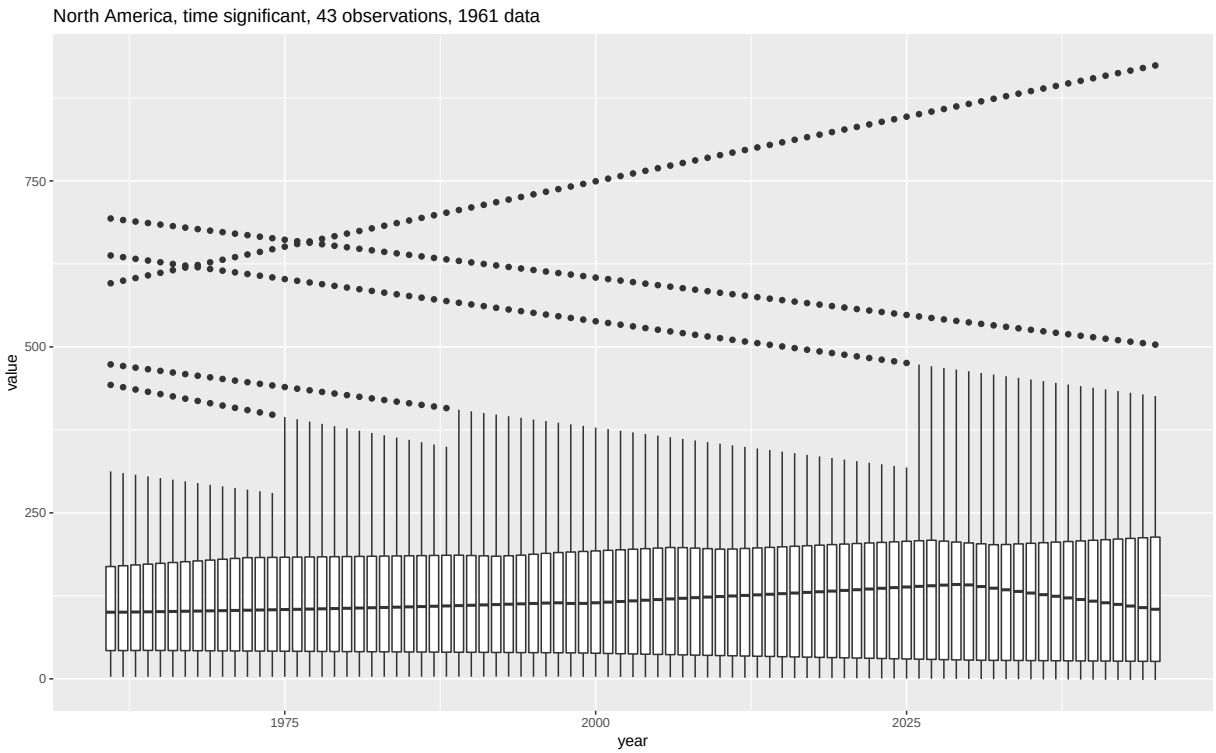

Figure 10: Box plot of the median, full model
The estimated median by year for the catchments in North America with a significant trend only in time, using the full model for the 1961-2010. This corresponds to 43 catchments in total.

4.2 Analysis of data from 1931-2010

4.2.1 Simple model

For the longer time series, it is reasonable to suspect that the proportion of significant trends will be higher. As can be seen in Table 5, this is the case. Once again, the number of significant trends is significantly higher than what would be expected. As always, we must be careful when interpreting the simple model, however due to the longer time scale, the risk of falsely interpreting the AMO and PDO as trends is lower.

Table 5: Results from the Simple Model 1931-2010

	# of catchments	# of significant trends	p-value	95% CI LB	95% CI UB
Europe	128	26	9.8574e-10	0.1334	0.2728
North America	194	24	4.4201e-4	0.0774	0.1700
Total	322	50	1.5726e-12	0.1157	0.1948

The significant trends are marked on a map in Figure 11. It appears the catchments with trends are more concentrated geographically, however that may be only due to the reduced number of catchments.

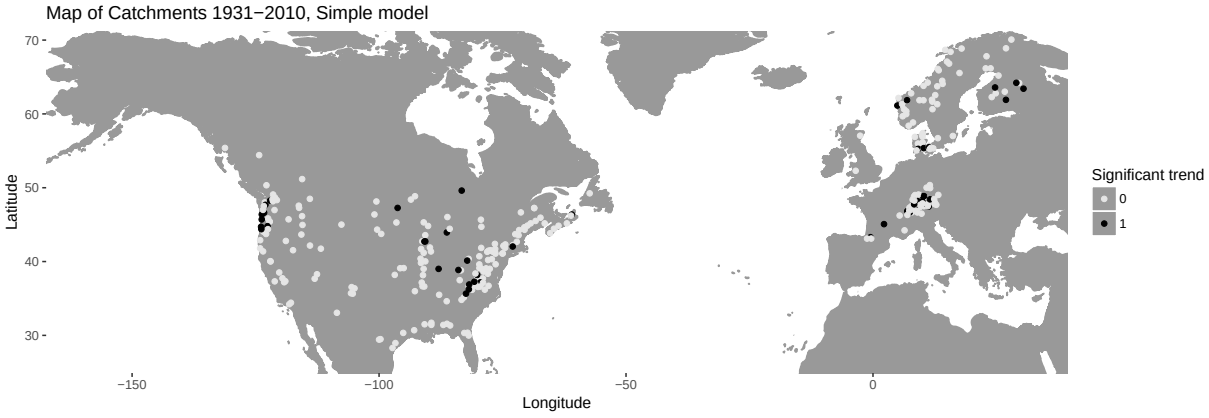

Figure 11: Significant catchments 1931-2010, simple model

The effects of the trend for the long time series can be found in Table 6. There doesn't appear to be any predictable way in which the trend affects the location parameter. There is still a significant relationship where the scale parameter increases with time for North America (p-value 0.0107). Now, however, the scale parameter in Europe decreases over time (p-value 0.0009). Since the results for Europe and North America point in different

directions, it might explain the lack of a consensus in the research, the trend affects different geographic areas differently.

Table 6: Simple model 1931-2010, direction of trends

	Increasing μ	Decreasing μ	Increasing σ	Decreasing σ
Europe	8	6	1	13
North America	8	7	9	1
Total	16	13	10	14

The effect of the significant trends on the parameters of the GEV. Note that the number of effects are greater than the number of significant trends, since for some catchments the trend affected both the location and scale parameters

The box plot showcasing the medians for the North American catchments with a significant trend in their GEV parameters for the simple model, using the 1931 data set is shown in Figure 12. The medians for the models based on the long time series behave similar to the models based on the short series. Once again, for individual catchments, the trend is pronounced, however since the trend affects each catchment differently, there is no overall pattern present. The pattern in North America is repeated in the European catchments. For all box plots using the 1931-2010 simple model, see Appendix B.3.

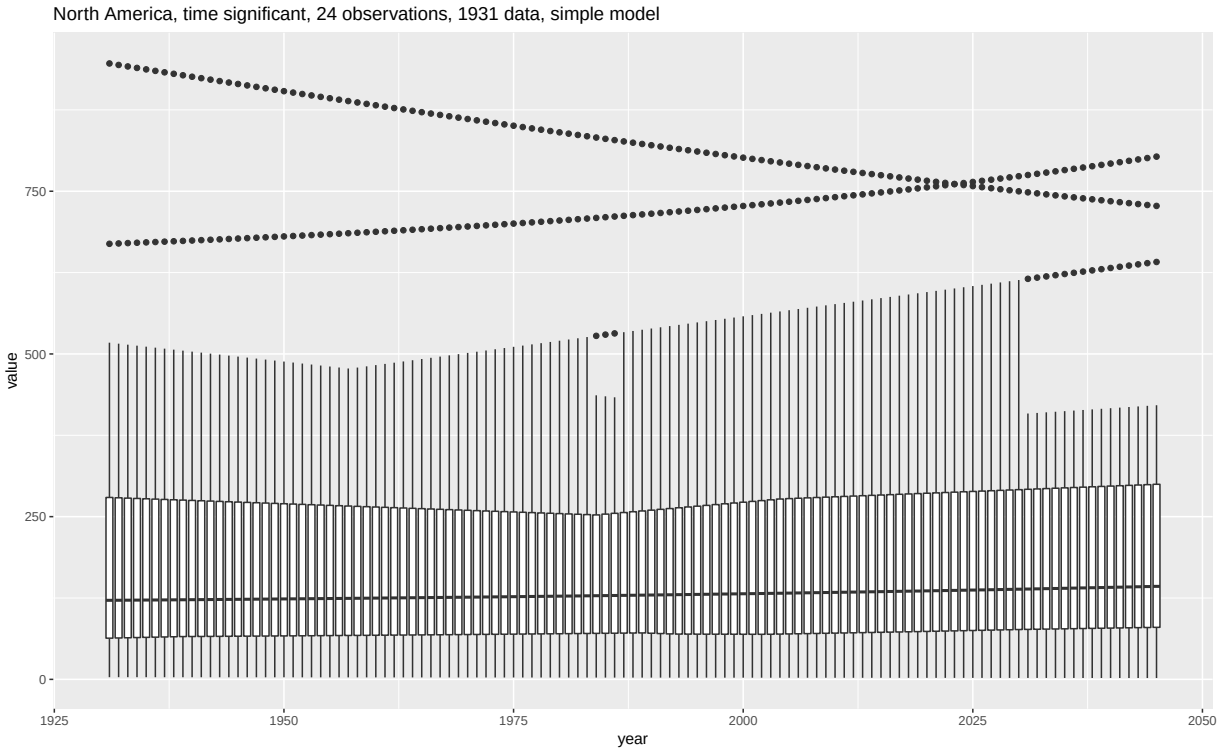

Figure 12: Box plot of the median, simple model

The estimated median by year for the catchments in North America with a significant trend in time, using the simple model for the 1931-2010. This corresponds to 24 catchments in total.

4.2.2 Full model

The results of the full model on the long time series can be found below, in Table 7. For the long model, there are no differences between the simple model and the full model, likely due to the reduced risk of misidentifying the effect of AMO or PDO as a trend.

Table 7: Results from the Full Model 1931-2010

	# of catchments	# of significant trends	p-value	95% CI LB	95% CI UB
Europe	128	26	9.8574e-10	0.1334	0.2728
North America	194	24	4.4201e-4	0.0774	0.1700
Total	322	50	1.5726e-12	0.1157	0.1948

A map of the significant catchments is found in Figure 13. There are no

changes from the simple model.

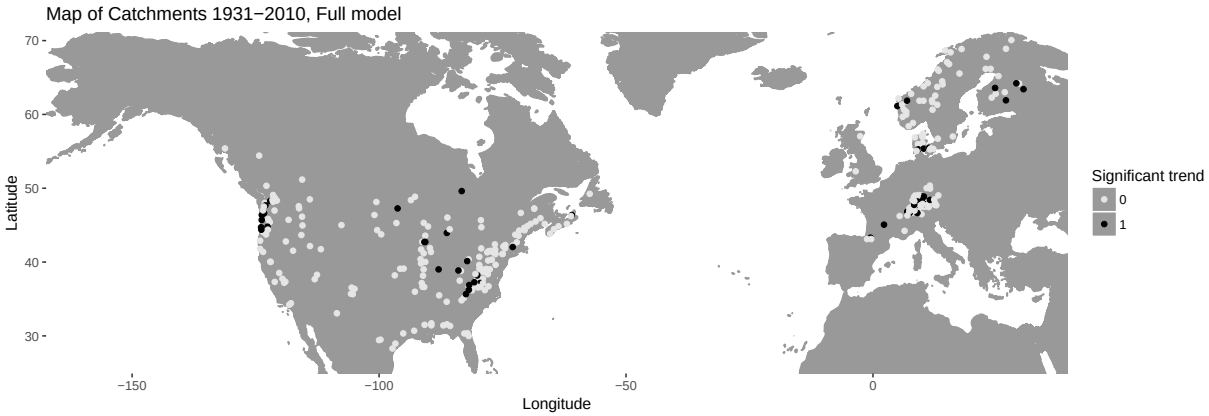

Figure 13: Significant catchments 1931-2010, full model

In Table 8, the effects of the trend for the full model are found. The results agree with the results from the simple model, only small differences are found, resulting in a lower p-value for the relationship between scale and time for Europe (p-value 0.0001).

Table 8: Full model 1931-2010, direction of trends

	Increasing μ	Decreasing μ	Increasing σ	Decreasing σ
Europe	8	8	0	13
North America	8	7	9	1
Total	16	15	9	14

The effect of the significant trends on the parameters of the GEV. Note that the number of effects are greater than the number of significant trends, since for some catchments the trend affected both the location and scale parameters

The median return levels for the North American catchments from 1931-2010 that were only dependent on time is shown in Figure 14. Once again, the results are that for each individual catchment, there exists a clear trend, but by looking at all the catchments together, this trend is eliminated. The results for those catchments that were dependent only on AMO/PDO mirrored these results for both Europe and North America.

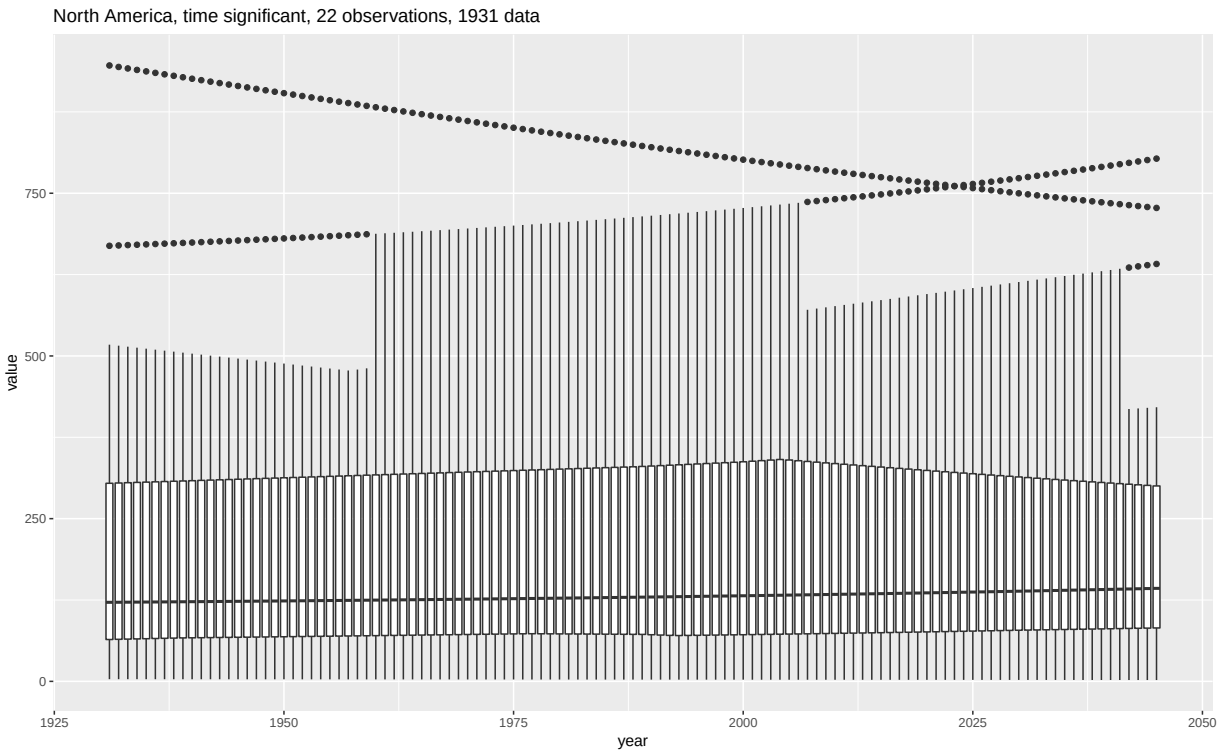

Figure 14: Box plot of the median, full model

The estimated median by year for the catchments in North America with a significant trend only in time, using the full model for the 1931-2010. This corresponds to 22 catchments in total.

For those catchments that were dependent on both time and AMO/PDO, however, there were evidence of shifts over time. The European catchments are illustrated in Figure 15. Here, there are large fluctuations from year to year, caused by yearly fluctuations in the AMO. Also, there appears to be a downward trend over time. However, since there are only 7 European catchments that are dependent on both time and AMO, these results are far from certain. For the North American catchments, the median return levels appear to increase over time, although there are very few observations. The box plot for the American catchments, as well as all other box plots for the full model are found in Appendix B.4.

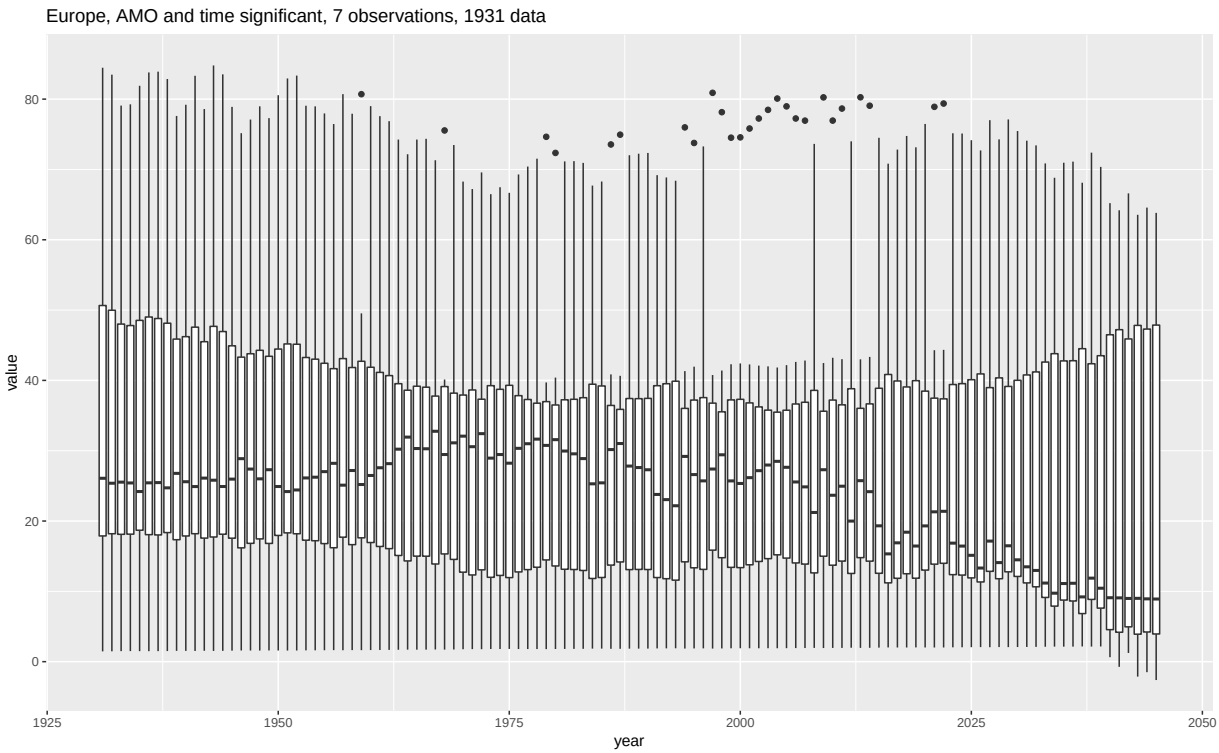

Figure 15: Box plot of the median, full model

The estimated median by year for the catchments in Europe with a significant trend both in time and AMO, using the full model for the 1931-2010. This corresponds to 7 catchments in total.

4.3 Conclusions

This study found a significant relationship between time and the parameters of the GEV distributions of the catchments. This result is in sharp contrast to the result arrived at by Hodgkins et al. [9]. This difference is likely due to the additional uncertainty introduced by modeling exceedances over estimated return levels. Indeed, when looking at the estimated median return levels, there were no clear trends.

Of particular interest is regional differences in the effect of time. While there were no such differences found for the location parameter, the scale parameter in North America was found to be increasing over time. There were also indications of a decreasing scale parameter in Europe, however, these results were only present in the long time series.

To illustrate the consequences of differences in scale, the densities of two artificial GEV distributions are shown in Figure 16. The GEV distribution with a higher scale parameter has a much higher probability for more severe events, as well as having larger variations from year to year, due to its flatter

density.

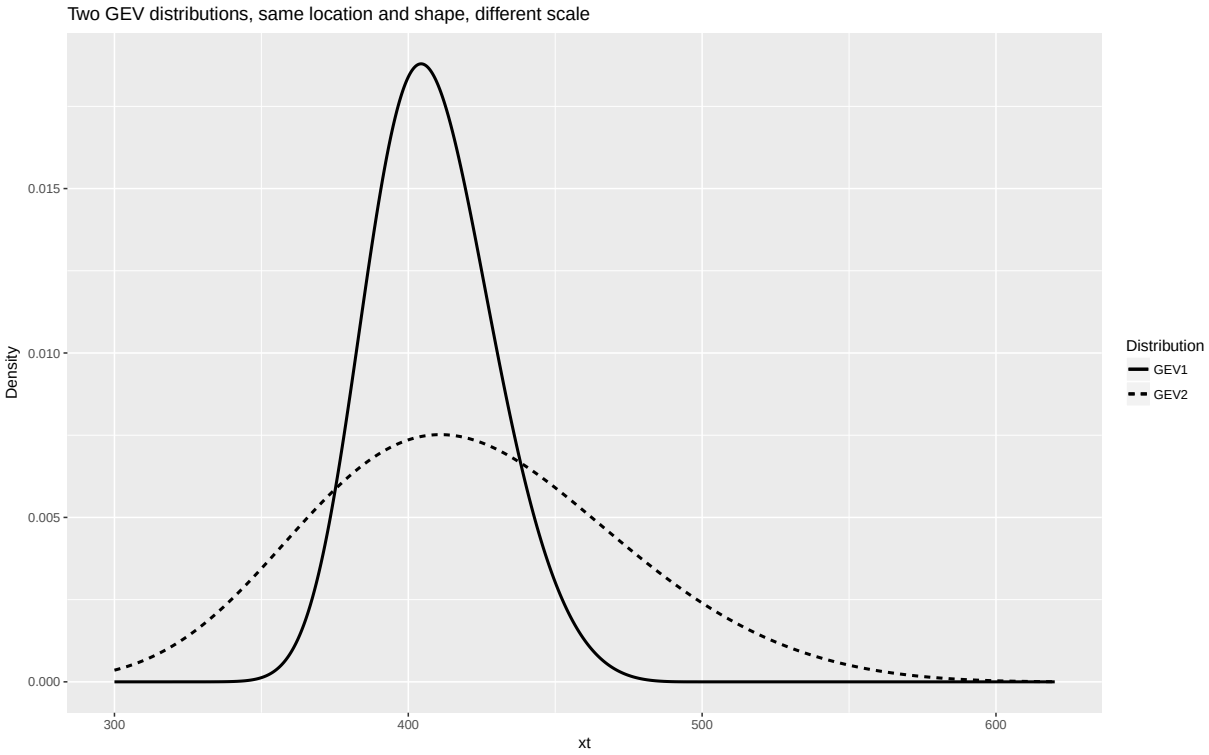

Figure 16: The density functions of two GEV distributions differing only in scale The parameters for GEV1 are $\mu = 400, \sigma = 20, \gamma = -0.2$ and the parameters of GEV2 are $\mu = 400, \sigma = 50, \gamma = -0.2$

However, despite the clear geographical divide between how the scale parameter was affected, no such effect was found on the median return levels. In fact, there were large differences between how catchments in the same continent were affected, suggesting that the patterns of flooding are more local than regional or global. Thus, one of the main conclusions must be that rather than modeling a large group of catchments, one must model each catchment separately.

This might also explain the difference between the results arrived at by Hodgkins et al. [9] and the results of this study. Since Hodgkins et al. focus on the return levels at a regional level, while this study focuses on the parameters of the GEV distribution itself at an individual level, it is reasonable to arrive at different results.

5 Summary and Concluding Remarks

The results of the study were very clear, there is a significant relationship between time and the dynamics of flooding that cannot be ignored. While there were several significant relationships between time and the location parameter in the respective GEV distributions, there were no clear geographical patterns. This likely means that the direction of shifts in the location parameter depend more on local circumstances than larger geographical factors.

For the scale parameter, however, there was a significant relationship between time and increasing scale parameter for North America. This relationship was significant for all models tested and for both time periods. For the European catchments, there was a significant relationship between time and decreasing scale parameter, but only for the long time series. Further research of this relationship is recommended.

When looking at return levels, no differences were found between the continents. There were large differences within the continents, suggesting that a local or individual approach is better than a regional. Though there was some evidence of regional trends in the median return level for the long time series, there were so few observations that the results may not be reliable.

During the course of the study a number of promising avenues for further research have presented themselves. If daily observations for the catchments were available, a Generalized Pareto distribution could be fitted to exceedances above a suitable threshold for each catchment. In general, fitting a GPD utilizes the data more effectively compared to fitting a GEV distribution to yearly maxima.

The results arrived at in this thesis can also be further examined. For instance, the Köppen-Geiger classicfication of climate zones can be used to see if there are any differences in the patterns of flooding between the climate zones.

The relationship between the AMO and time, as well as the relationship between the PDO and time could be modeled in order to achieve better predictions of future return levels. A better classification of which catchments are affected by the AMO and which are affected by the PDO would also be a welcome improvement.

Another area of possible improvement is using a different index than the PDO. Since there doesn't exist any clear evidence between the PDO and flooding in North America, perhaps another index could be chosen to better model the Pacific Ocean. In particular the El Niño-Southern Oscillation (ENSO) could be used. While mainly concentrated in the South Pacific, the ENSO affects the whole region, and thus could be suitable for further study.

References

[1] Tim Appelhans, Florian Detsch, Christoph Reudenbach, and Stefan Woellauer. *mapview: Interactive Viewing of Spatial Data in R*, 2018. R package version 2.3.0.

[2] Winston Chang. *webshot: Take Screenshots of Web Pages*, 2017. R package version 0.5.0.

[3] J.H. Christensen, K. KrishnaKumar, E. Aldrian, S.-I. An, I.F.A. Cavalcanti, M. deCastro, W. Dong, P. Goswami, A. Hall, J.K. Kanyanga, A. Kitoh, J. Kossin, N.-C. Lau, J. Renwick, D.B. Stephenson, S.-P. Xie, and T. Zhou. *Climate Phenomena and their Relevance for Future Regional Climate Change*, book section 14, page 1217–1308. Cambridge University Press, Cambridge, United Kingdom and New York, NY, USA, 2013.

[4] Original S code by Richard A. Becker and Allan R. Wilks. R version by Ray Brownrigg. *mapdata: Extra Map Databases*, 2018. R package version 2.3.0.

[5] S. Coles. *An Introduction to Statistical Modeling of Extreme Values*. Springer Series in Statistics. Springer London, 2011.

[6] David B. Enfield, Alberto Mestas-Nunez, and Paul Trimble. The atlantic multidecadal oscillation and its relation to rainfall and river flows in the continental u.s. 28, 05 2001.

[7] Eric Gilleland and Richard W. Katz. extRemes 2.0: An extreme value analysis package in R. *Journal of Statistical Software*, 72(8):1–39, 2016.

[8] D.L. Hartmann, A.M.G. Klein Tank, M. Rusticucci, L.V. Alexander, S. Brönnimann, Y. Charabi, F.J. Dentener, E.J. Dlugokencky, D.R. Easterling, A. Kaplan, B.J. Soden, P.W. Thorne, M. Wild, and P.M. Zhai. *Observations: Atmosphere and Surface*, book section 2, page 159–254. Cambridge University Press, Cambridge, United Kingdom and New York, NY, USA, 2013.

[9] Glenn A. Hodgkins, Paul H. Whitfield, Donald H. Burn, Jamie Hannaford, Benjamin Renard, Kerstin Stahl, Anne K. Fleig, Henrik Madsen, Luis Mediero, Johanna Korhonen, Conor Murphy, and Donna Wilson. Climate-driven variability in the occurrence of major floods across north america and europe. *Journal of Hydrology*, 552:704 – 717, 2017.

[10] M. Ross Leadbetter, Georg Lindgren, and Holger Rootzén. *Extremes and related properties of random sequences and processes*. Springer Series in Statistics. Springer, 1983.

[11] MacDonald Glen M. and Case Roslyn A. Variations in the pacific decadal oscillation over the past millennium. *Geophysical Research Letters*, 32(8).

[12] R Core Team. *R: A Language and Environment for Statistical Computing*. R Foundation for Statistical Computing, Vienna, Austria, 2017.

[13] Hadley Wickham. *ggplot2: Elegant Graphics for Data Analysis*. Springer-Verlag New York, 2009.

A Distributions and tests

In this appendix, some necessary distributions and tests are defined. These are the binomial distribution, the χ^2-distribution, and the Likelihood Ratio test. Their definitions are found in Definition A.1, Definition A.2, and Theorem A.1, respectively.

Definition A.1 (Binomial distribution) *Let X be a random variable. If its probability mass function is given by:*

$$P(X = k) = \binom{n}{k} p^k (1-p)^{n-k} \qquad for \;\; k = 0, 1, 2, \ldots, n$$

then X has a binomial distribution with parameters $n \in \mathbb{N}, p \in [0, 1]$

Definition A.2 (χ^2-distribution) *Let X be a random variable. If its probability density function is given by:*

$$f(x) = \frac{1}{2^{k/2}\Gamma(k/2)} x^{k/2-1} e^{-x/2} \qquad for \;\; x > 0$$

then X is χ^2 distributed with $k \in \mathbb{N}$ degrees of freedom.

Theorem A.1 (Likelihood Ratio test) *Let M_1 be a model with parameter vector $\boldsymbol{\theta}_1 = \left(\boldsymbol{\theta}^{(0)}, \boldsymbol{\theta}^{(1)}\right)$ and let M_0 be a submodel with parameter vector $\boldsymbol{\theta}_0 = \left(\boldsymbol{\theta}^{(0)}, \boldsymbol{\theta}^{(1)}\right)$ under the restriction that the k-dimensional subvector $\boldsymbol{\theta}^{(1)} = \mathbf{0}$. Further, let $\ell_0(M_0)$ and $\ell_1(M_1)$ be the maximized log-likelihood for the respective models.*

Then, under the null hypothesis $H_0 : \boldsymbol{\theta}^{(1)} = \mathbf{0}$, the deviance statistic

$$D = 2\left(\ell_1(M_1) - \ell_0(M_0)\right)$$

will be $\chi^2(k)$-distributed[5, p.34-35].

B Box plots of the estimated median

B.1 1961 data, simple model

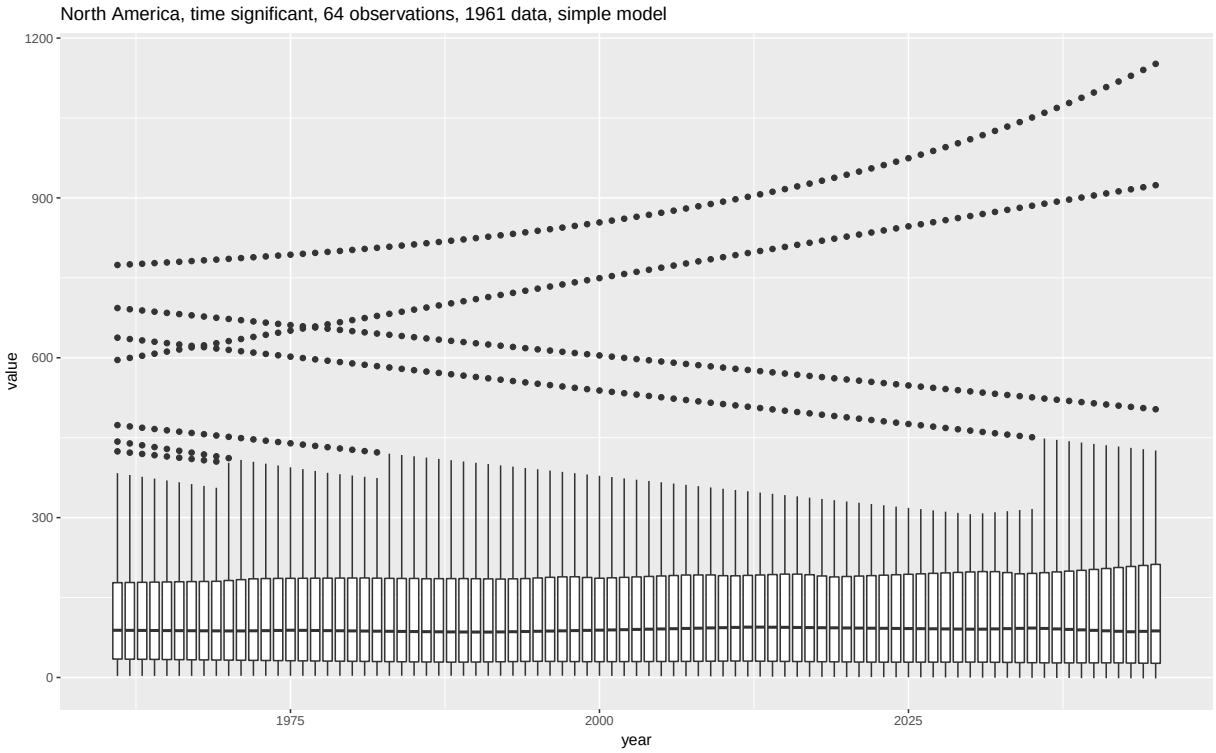

Figure 17: Box plot of the median, simple model
The estimated median by year for the catchments in North America with a significant trend in time, using the simple model for the 1961-2010. This corresponds to 64 catchments in total.

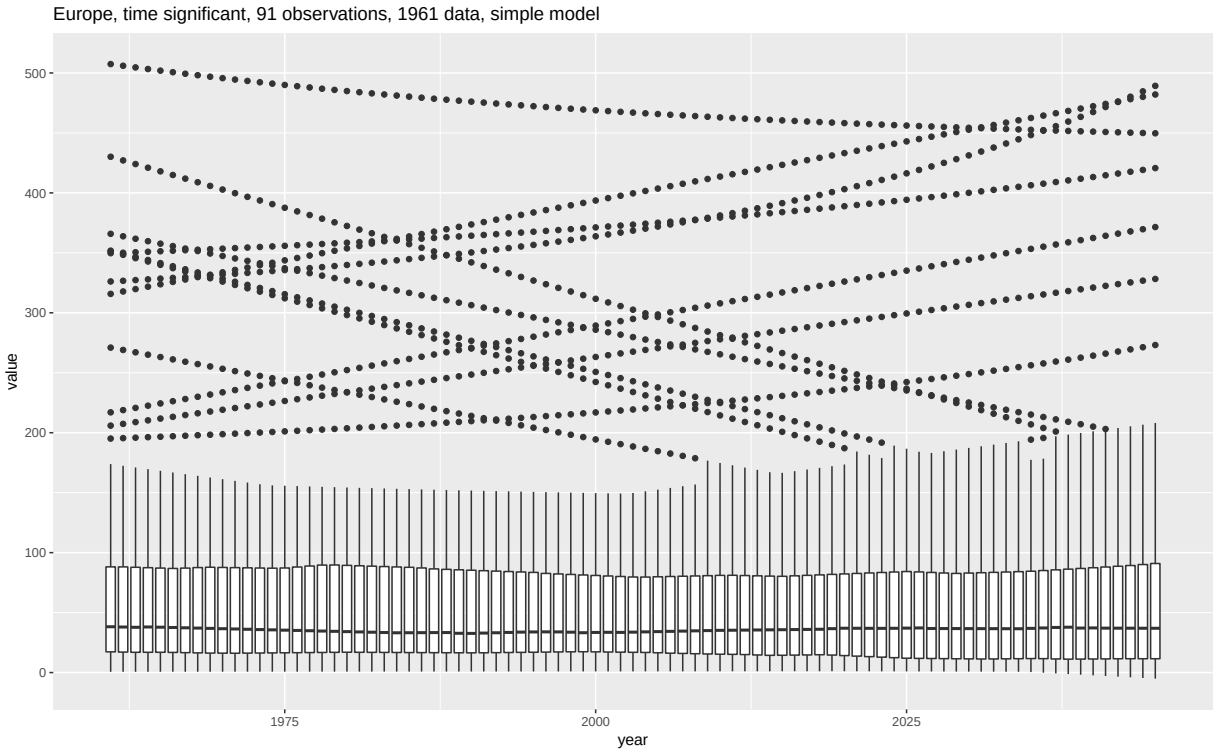

Figure 18: Box plot of the median, simple model
The estimated median by year for the catchments in Europe with a significant trend in time, using the simple model for the 1961-2010. This corresponds to 91 catchments in total.

B.2 1961 data, full model

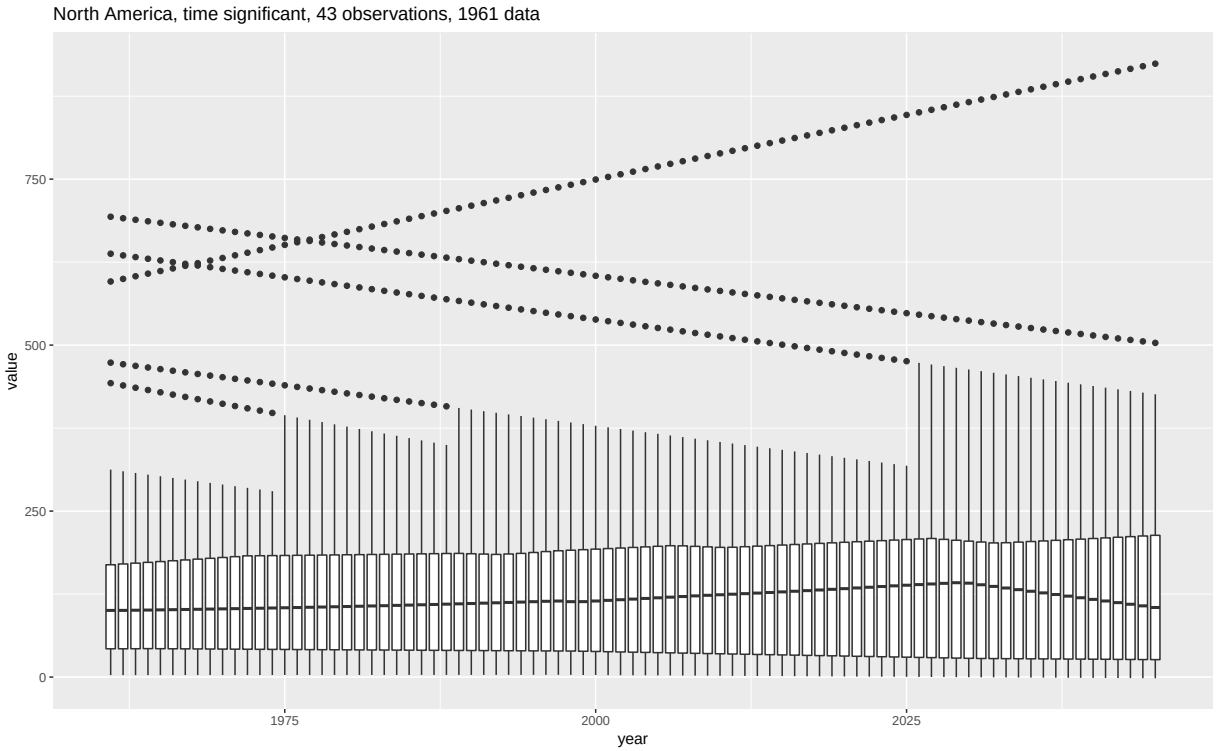

Figure 19: Box plot of the median, full model
The estimated median by year for the catchments in North America with a significant trend only in time, using the full model for the 1961-2010. This corresponds to 43 catchments in total.

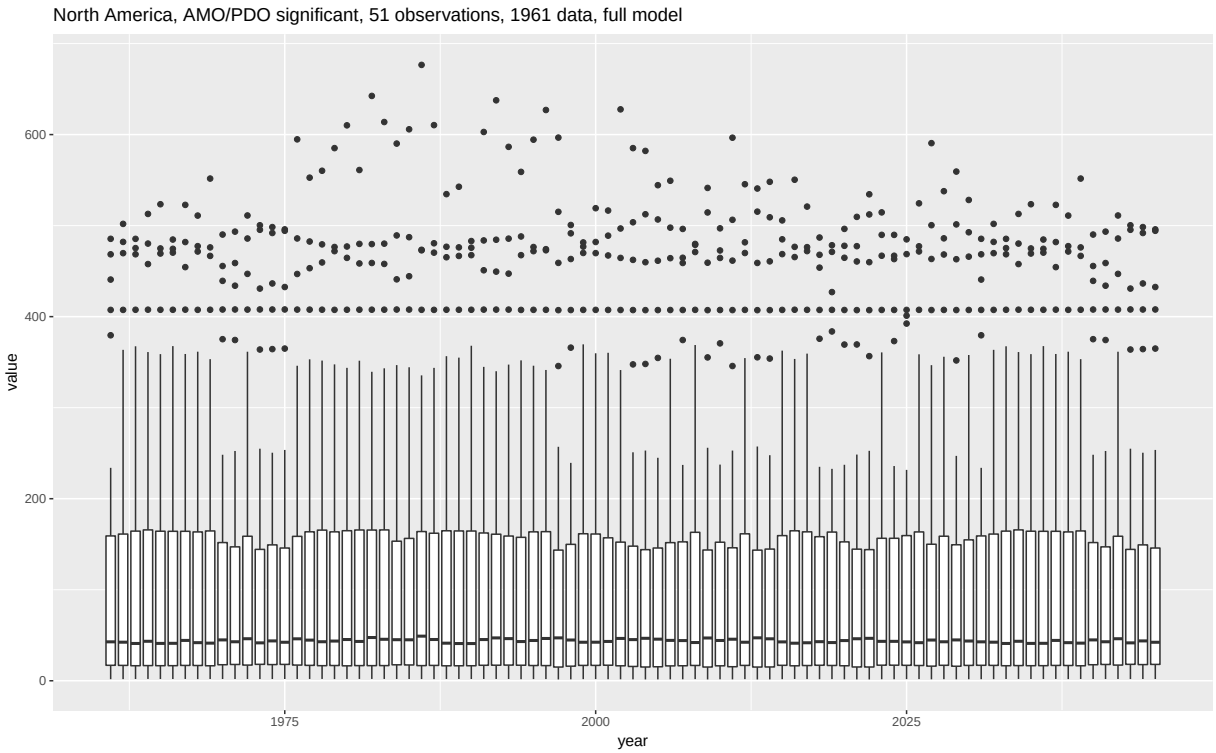

Figure 20: Box plot of the median, full model
The estimated median by year for the catchments in North America with a significant trend only in AMO/PDO, using the full model for the 1961-2010. This corresponds to 51 catchments in total.

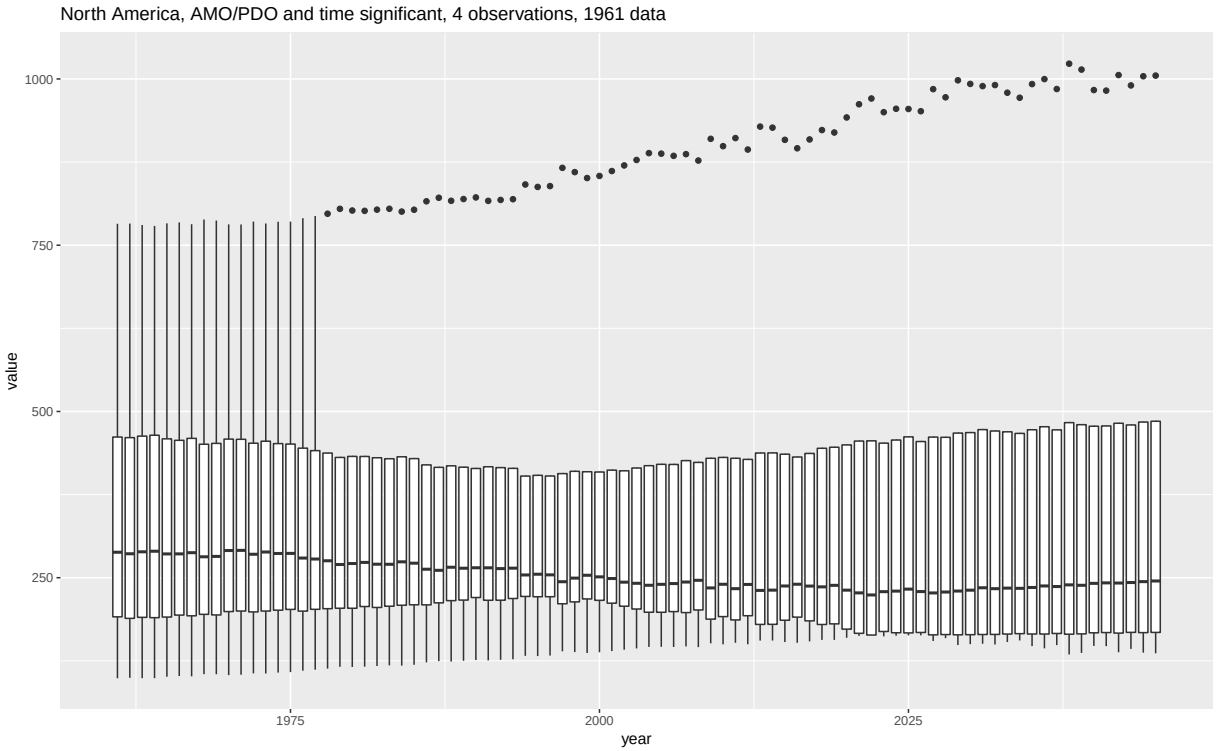

Figure 21: Box plot of the median, full model
The estimated median by year for the catchments in North America with a significant trend both in time and in AMO/PDO, using the full model for the 1961-2010. This corresponds to 4 catchments in total.

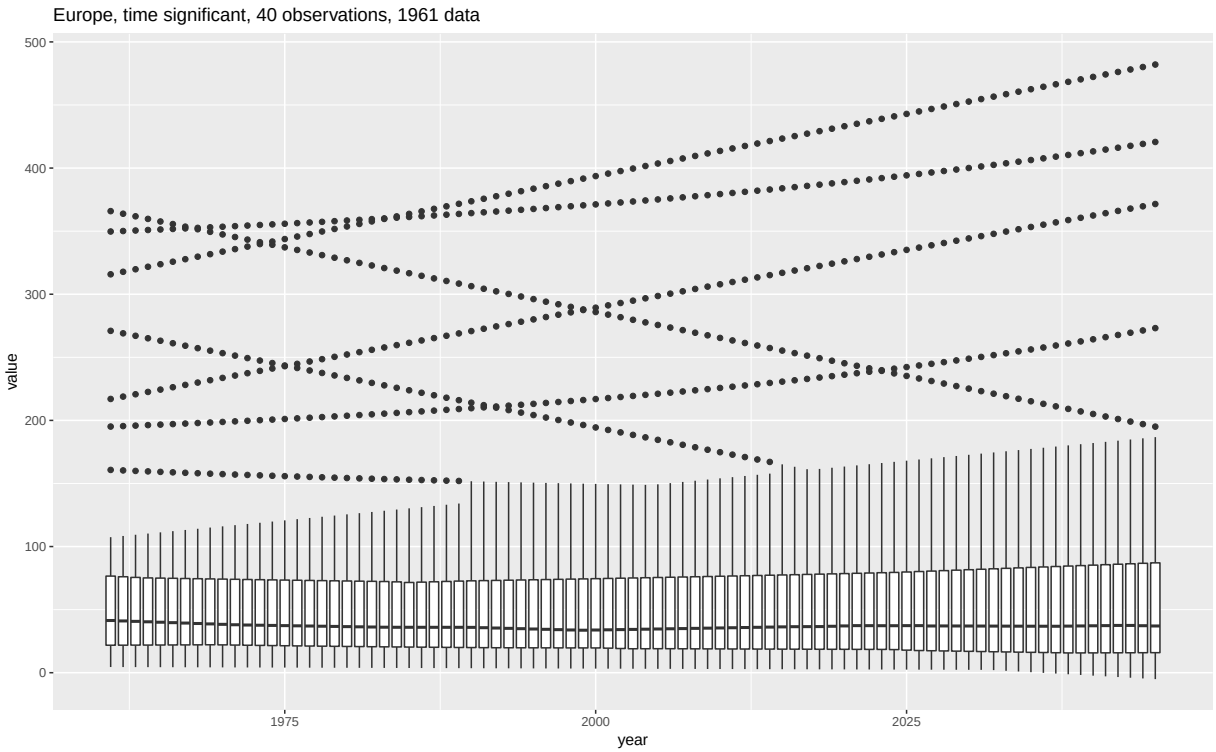

Figure 22: Box plot of the median, full model
The estimated median by year for the catchments in Europe with a significant trend only in time, using the full model for the 1961-2010. This corresponds to 40 catchments in total.

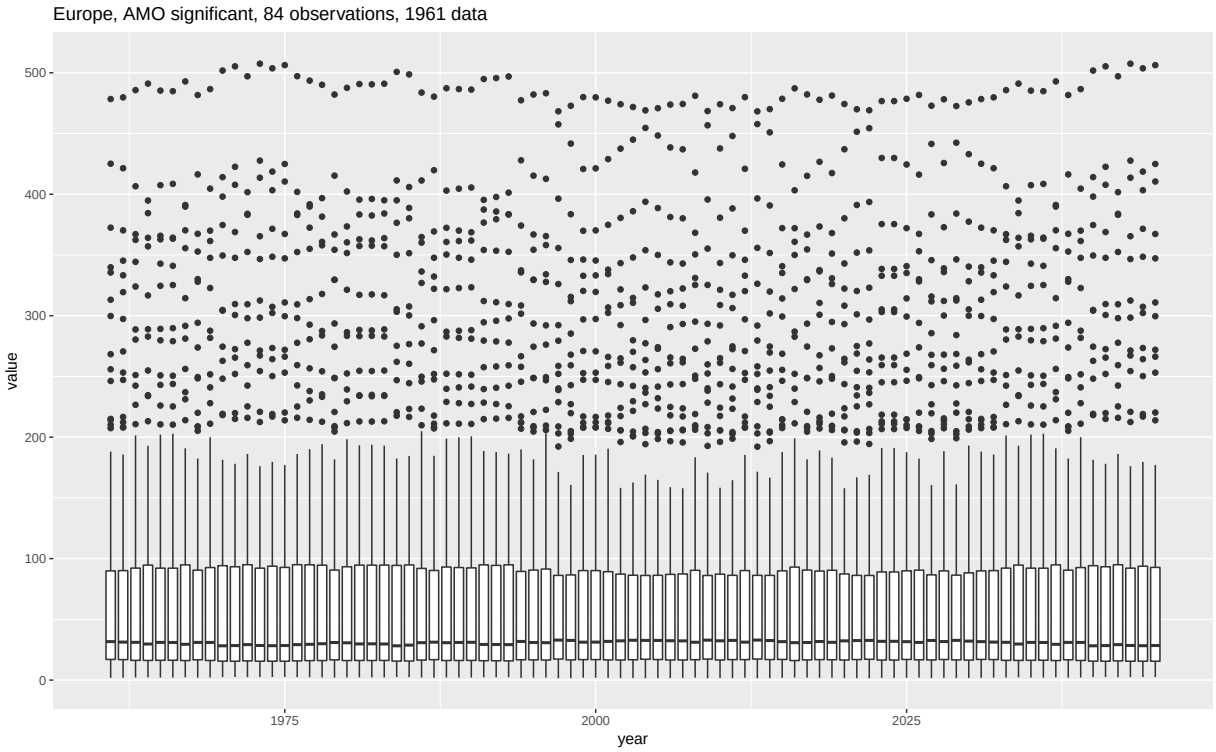

Figure 23: Box plot of the median, full model

The estimated median by year for the catchments in Europe with a significant trend only in AMO, using the full model for the 1961-2010. This corresponds to 84 catchments in total.

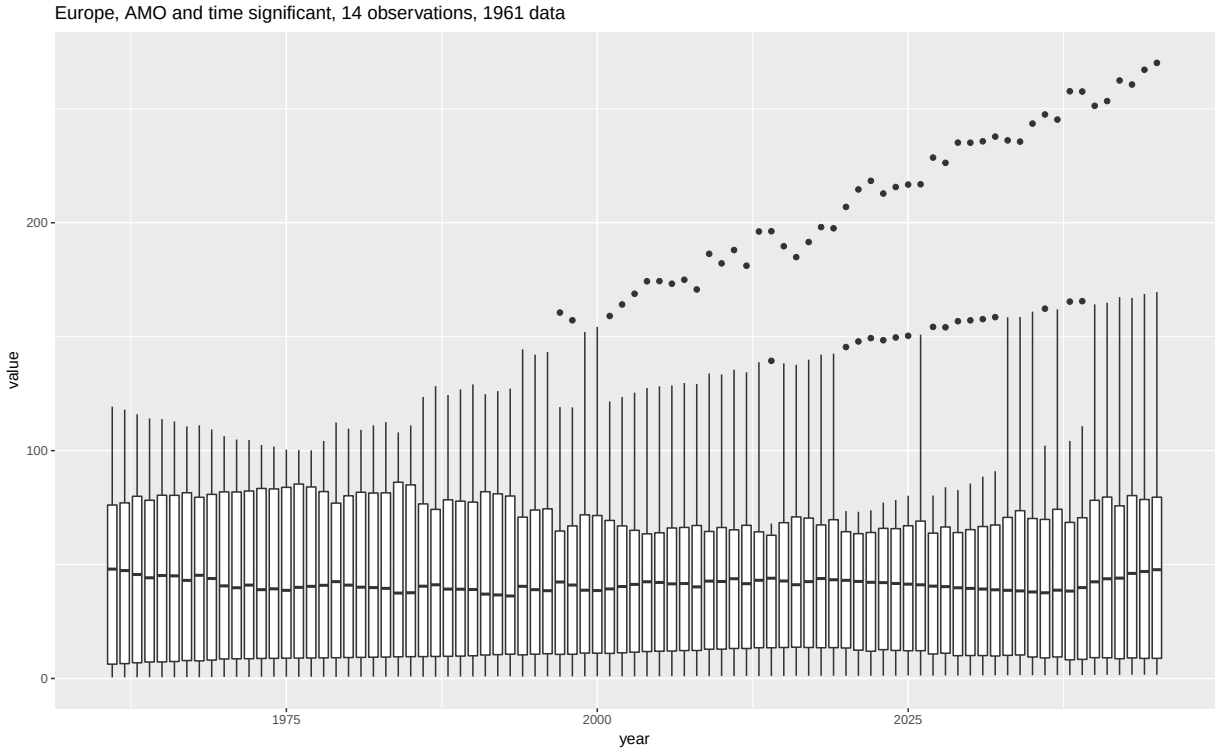

Figure 24: Box plot of the median, full model

The estimated median by year for the catchments in Europe with a significant trend both in time and in AMO, using the full model for the 1961-2010. This corresponds to 14 catchments in total.

B.3 1931 data, simple model

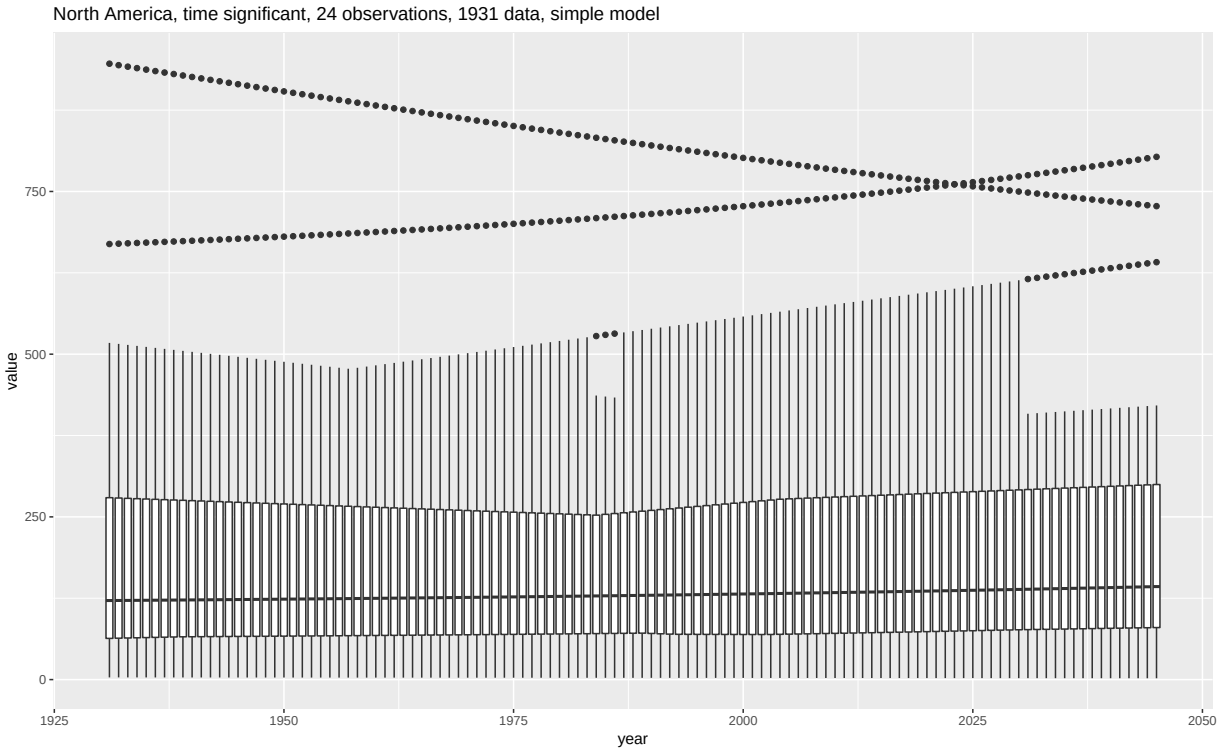

Figure 25: Box plot of the median, simple model
The estimated median by year for the catchments in North America with a significant trend in time, using the simple model for the 1931-2010. This corresponds to 24 catchments in total.

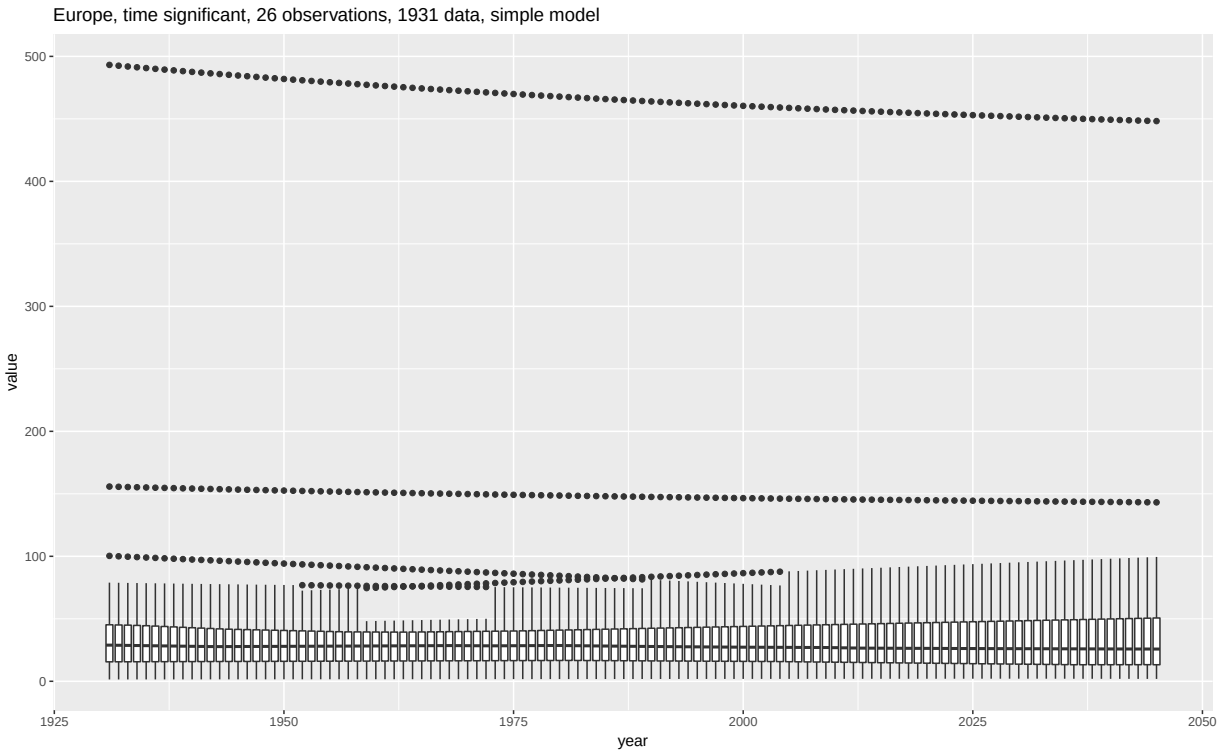

Figure 26: Box plot of the median, simple model
The estimated median by year for the catchments in Europe with a significant trend in time, using the simple model for the 1931-2010. This corresponds to 26 catchments in total.

B.4 1931 data, full model

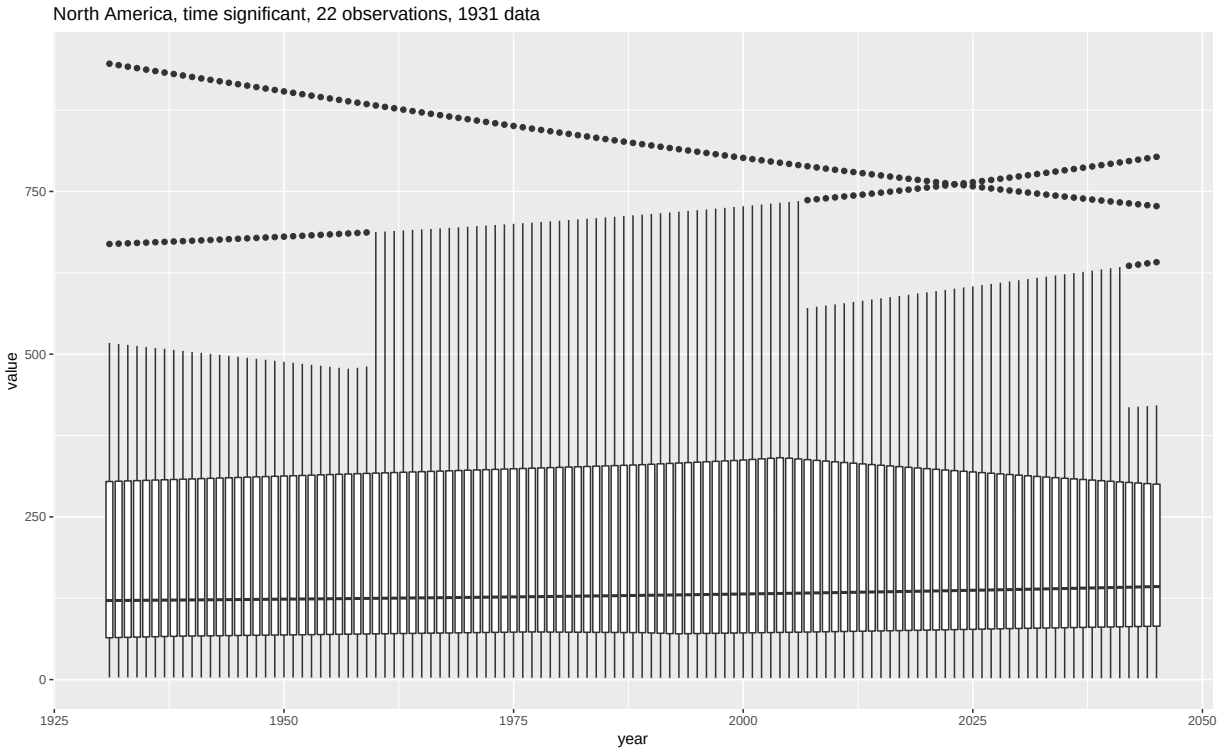

Figure 27: Box plot of the median, full model
The estimated median by year for the catchments in North America with a significant trend only in time, using the full model for the 1931-2010. This corresponds to 22 catchments in total.

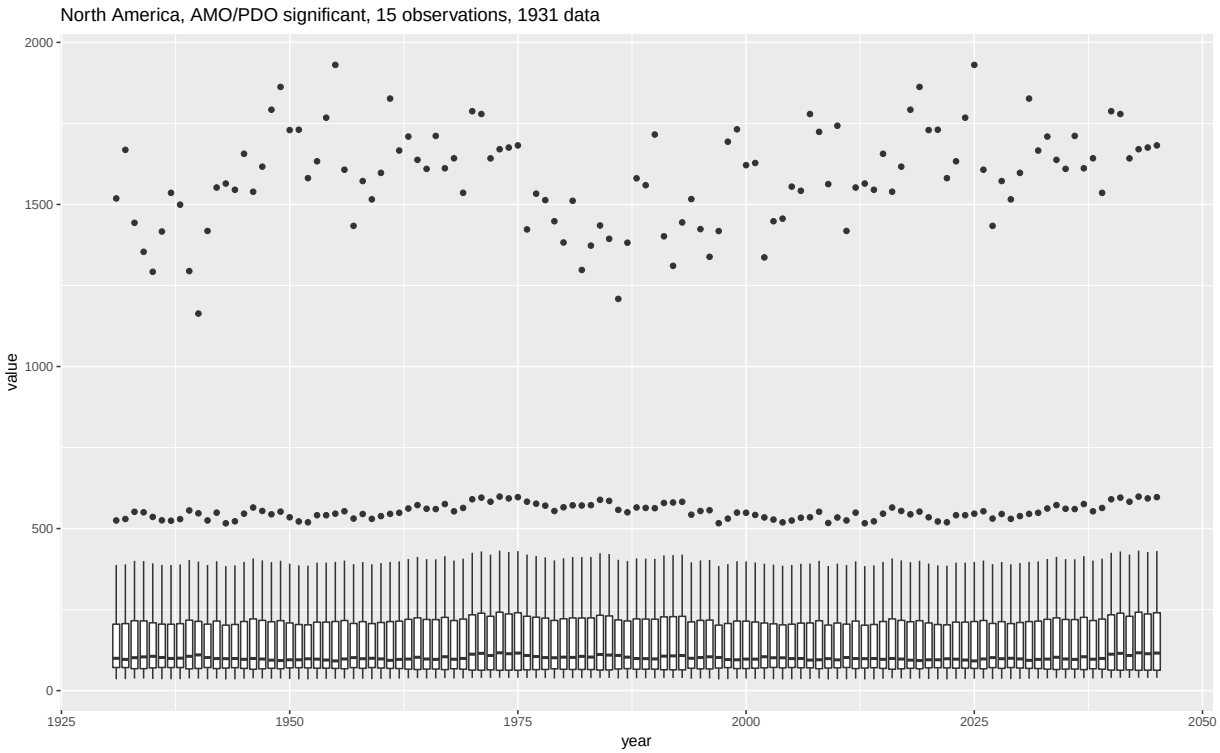

Figure 28: Box plot of the median, full model
The estimated median by year for the catchments in North America with a significant trend only in AMO/PDO, using the full model for the 1931-2010. This corresponds to 15 catchments in total.

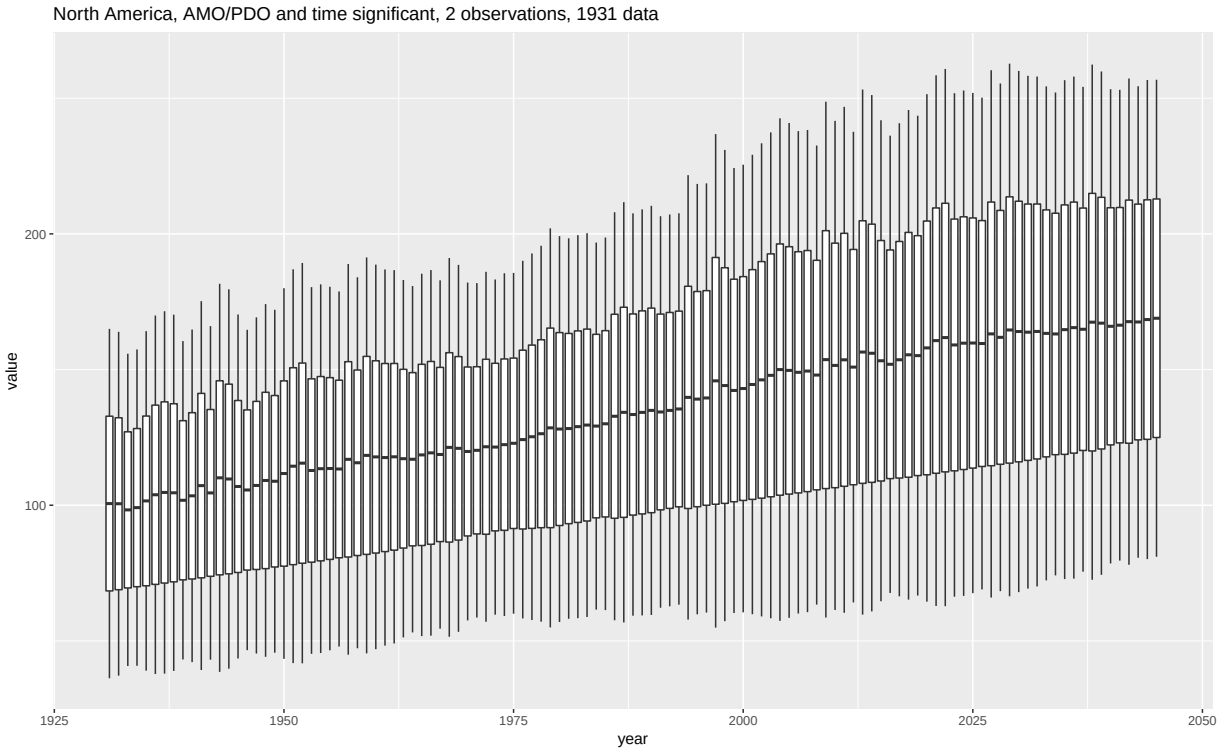

Figure 29: Box plot of the median, full model

The estimated median by year for the catchments in North America with a significant trend both in time and AMO/PDO, using the full model for the 1931-2010. This corresponds to 2 catchments in total.

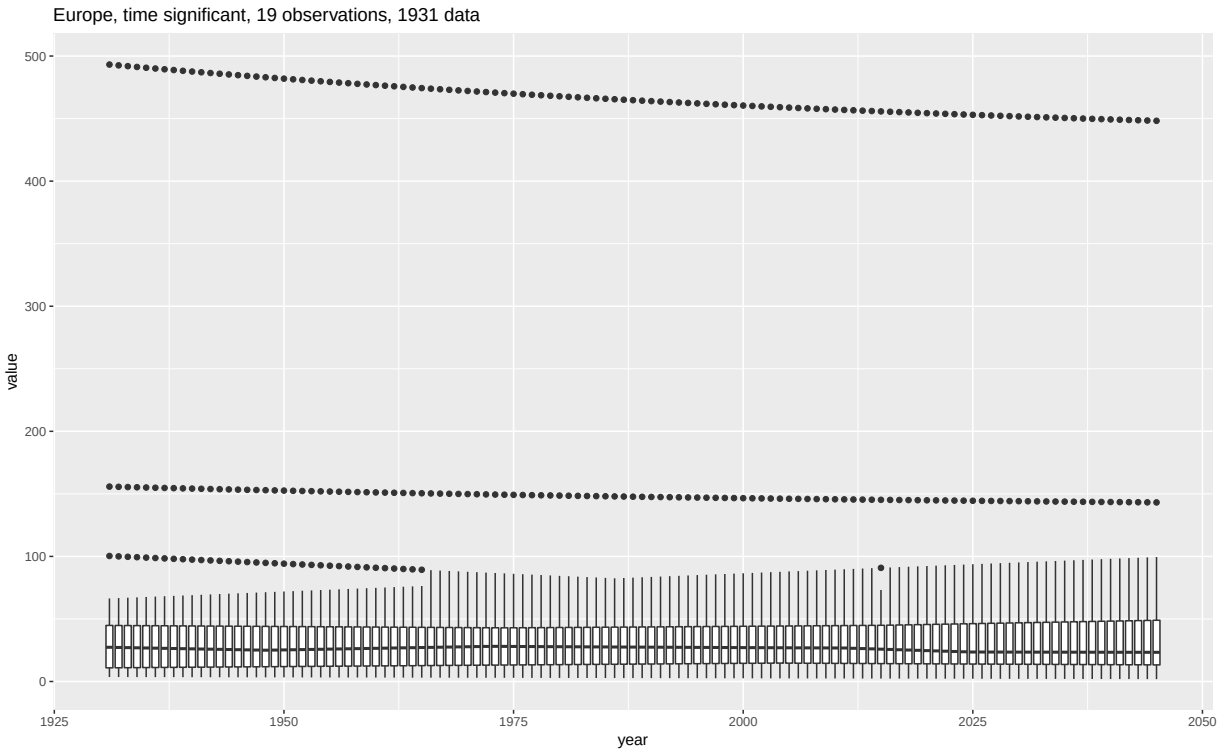

Figure 30: Box plot of the median, full model

The estimated median by year for the catchments in Europe with a significant trend only in time, using the full model for the 1931-2010. This corresponds to 19 catchments in total.

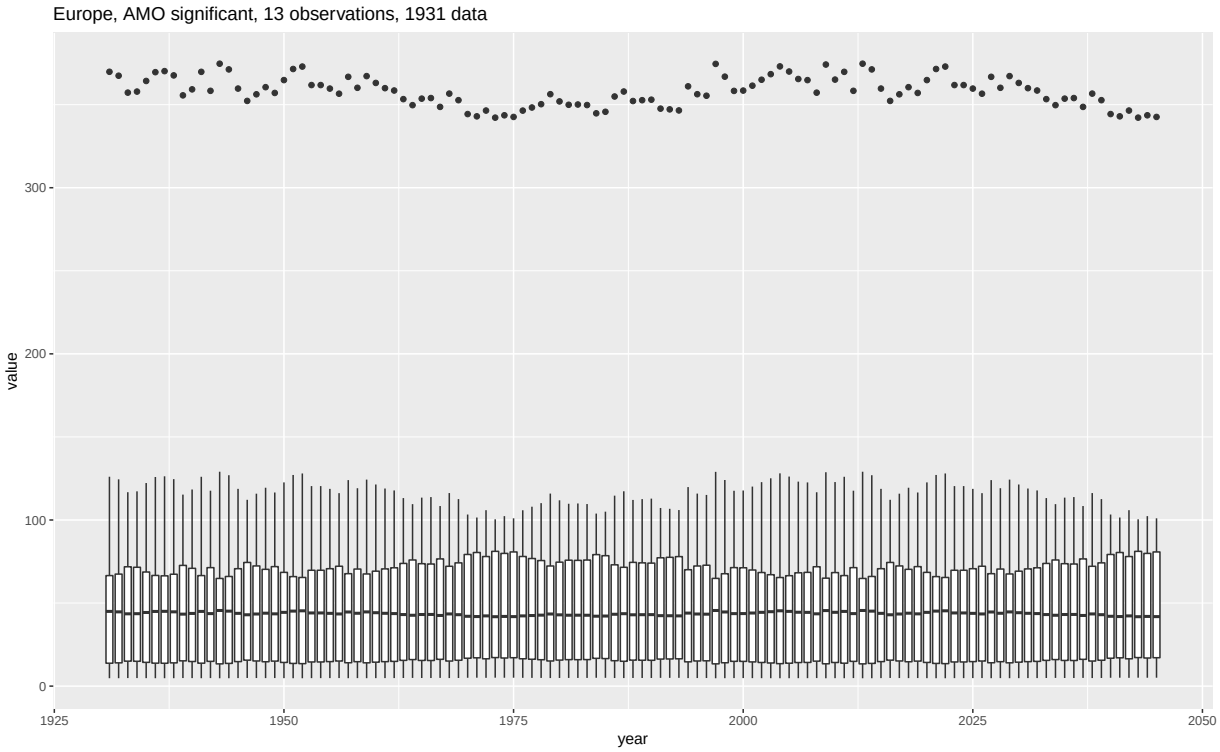

Figure 31: Box plot of the median, full model

The estimated median by year for the catchments in Europe with a significant trend only in AMO, using the full model for the 1931-2010. This corresponds to 13 catchments in total.

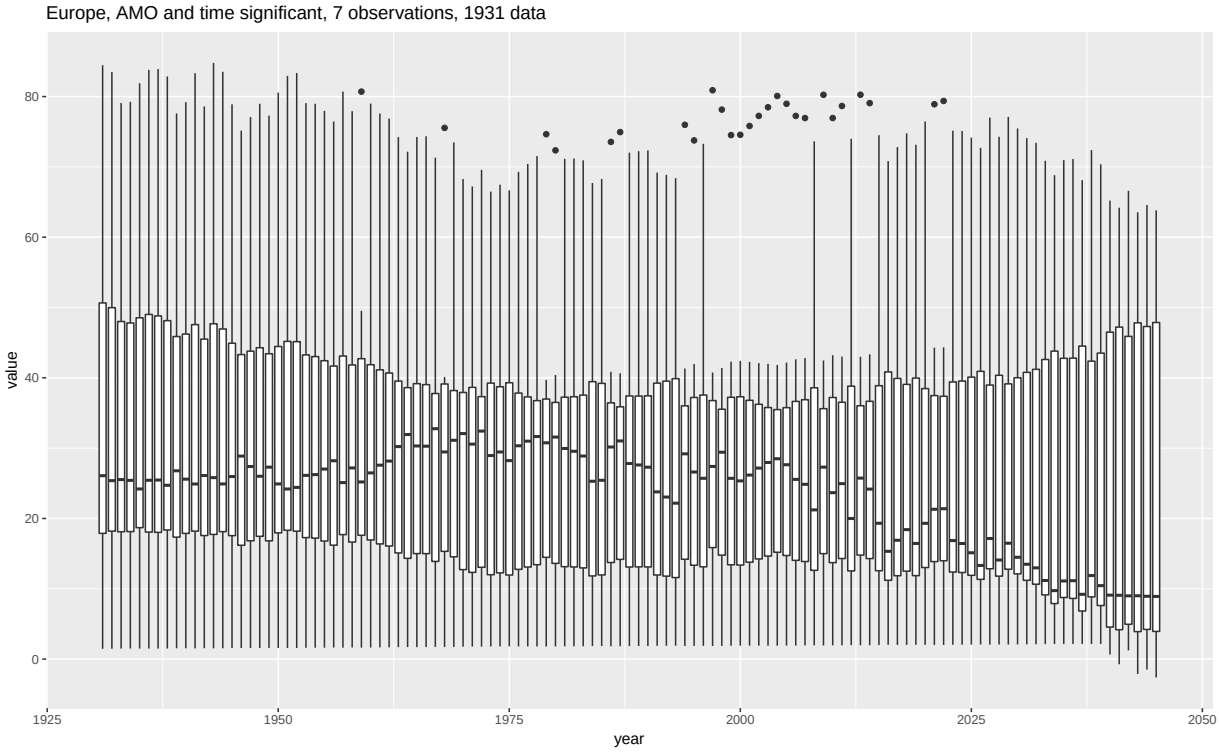

Figure 32: Box plot of the median, full model

The estimated median by year for the catchments in Europe with a significant trend both in time and AMO, using the full model for the 1931-2010. This corresponds to 7 catchments in total.